Phylogenetic Relationships and the Evolution of Fin and Body Shape in the Surgeonfishes

Linnea L. Lungstrom[1,2], Mireille Farjo[3], Ryan Isdonas[3], Andrew B. George[2,4], & Mark W. Westneat[1,2,3,4]

[1]Committee on Evolutionary Biology, University of Chicago, Chicago, IL 60637, USA

[2]Division of Fishes (IRC), Field Museum of Natural History, 1400 S Dusable Lake Shore Drive, Chicago, Illinois. 60605 USA

[3]The College, University of Chicago, Chicago, IL 60637, USA

[4]Department of Organismal Biology and Anatomy, University of Chicago, Chicago, IL 60637, USA

Keywords: Acanthuridae, phylogenetics, morphometrics, locomotion, integration, evolution

Highlights:

- Improved, nearly complete phylogeny of surgeonfishes (family Acanthuridae).
- Novel method to accurately account for phylogenetic covariation among shapes.
- Head and body shape of surgeonfishes are significantly related to diet.
- Fishes exhibit pairs of high/low aspect ratio propulsive fins (caudal and pectoral).
- Caudal fins have the highest evolutionary rates and covary with both the body and pectoral fin.

Abstract

Patterns of evolutionary change in the fin and body shapes of fishes are strongly related to dietary ecology and locomotor mechanisms, and associations between shapes affects ecomorphological relationships between functional groups and evolutionary rates across taxa. The surgeonfishes (Acanthuridae), a group of 83 species across 6 genera, show high diversity in head, body, and propulsive fin (caudal and pectoral) shape, suggesting that morphometric analysis of these functionally relevant traits may provide insight into the ecomorphology and evolutionary history of this important fish family. Here, we develop a new multi-locus, time-calibrated phylogenetic hypothesis for the surgeonfishes based on 19 loci for 80 acanthurid species and 45 outgroups. Detailed head, body, and fin geometric morphometric data were collected for all 80 surgeonfish species in the tree, and patterns of shape evolution across the family were visualized using phylomorphospaces. We used a three-state feeding trait axis across the herbivore to planktivore continuum to examine how morphometric shape relates to diet. Head and body shape were significantly associated with diet. Additionally, species exhibited two alternative locomotor strategies: high aspect ratio (AR) tails were associated with low AR pectoral fins, slender bodies, and pelagic planktivory, whereas species with low AR tail fins had wing-like, high AR pectoral fins, deeper bodies, and were mostly benthic grazers. Using a novel phylogenetic comparative method to investigate evolutionary correlations between shapes, we found that the caudal fin had the highest evolutionary rates and covaried with both the body and pectoral fin, likely due to dietary and locomotor demands, respectively.

1. Introduction

Ecomorphological studies provide critical insight into how the interaction between an organism's morphology and its ecology relates to the adaptive diversification and survival of species. Previous work has established many ecomorphological relationships along the benthic-pelagic axis in marine fishes as head and body characteristics (Friedman et al., 2016, 2019; Tavera et al., 2018) as well as functional jaw mechanics (Cooper et al., 2017) are associated with habitat. Habitat use is also linked to swimming mechanics and locomotor mode (Fulton et al., 2001), which can have their own associations with specific body forms (Collar et al., 2009; Friedman et al., 2021; Walker et al., 2013) and fin shapes (Walker & Westneat, 2002; Webb, 1984; Westneat, 1996). These strong relationships between shape, habitat, and functional performance influence evolutionary rates among marine fishes. Body shapes (Price et al., 2019) and, to a lesser extent, fin shapes (Du et al., 2019), have been shown to evolve at different rates across fishes. Additionally, locomotor mode and transitions across the benthic-pelagic axis, especially when related to dietary ecotype, have been associated with selective evolutionary regimes and differences in rates of evolution (Friedman et al., 2016; McCord et al., 2021; Ribeiro et al., 2018, Santaquiteria et al., 2025).

While the majority of the literature focuses on the ecomorphological relationships of individual body parts (e.g., head, bodies, or fins) and their influence on evolutionary rates, some work has also been done to look at how shape variation in these structures may covary with one another in the context of morphological, ecological, or behavioral diversification (Aguilar-Medrano et al., 2016; Feilich, 2016; Goswami & Polly, 2010; Larouche et al., 2015, 2018). Covariation of shape has also been suggested to influence adaptive diversification as both a constraint and facilitator of evolution (Du et al., 2019; Evans et al., 2017; Goswami et al., 2014;

Goswami & Polly, 2010; Klingenberg, 2013; Wagner & Altenberg, 1996). With a robust morphometric dataset and well-resolved phylogeny, we can ask nuanced questions related to covariation between shapes through both ecomorphological and evolutionary lenses. For example, are body forms, like pectoral and caudal fin shape, more correlated with one another than head or body shape? Does the degree of shape correlation between body forms relate to fishes' ecological niche and/or behavior? To what extent do the shared evolutionary histories of species explain similar patterns of covariation between shapes, and are the rates of morphometric evolution different or similar depending on the strength of association between shapes? Current tools to investigate these questions about shape covariation assume a Brownian motion (BM) model of evolution (Adams et al., 2025; Baken et al., 2021) which is problematic for systems in which some mode of selection is acting on shape (Monteiroa, 2013; Revell, 2010). Here, we implement novel phylogenetic comparative methodology to accurately account for phylogenetic signal when looking at shape covariation within the surgeonfishes (Acanthuridae), in the context of a new multi-locus, time-calibrated phylogeny.

Surgeonfishes are an ideal family of fishes in which to investigate these ecomorphological and shape covariation questions as they vary widely in head, body, and fin shape, as well as feeding and locomotor modes. Surgeonfishes are found globally, with body shapes ranging from deep and rotund to shallow and elongated. Their fins also vary in shape and use; some surgeonfishes locomote via their caudal fin while others primarily use their pectoral fins to swim. Surgeonfishes' dietary ecotypes range from benthic herbivores, which graze on algae, to pelagic planktivores, with some species exhibiting omnivory (Clements et al., 2003; Winterbottom, 1971). Linear morphometric measurements of surgeonfishes paired with evolutionary modeling have shown that head and body shapes are associated with different

dietary guilds, suggesting that ecomorphological evolution is consistent with adaptive dynamics in this clade (Friedman et al., 2016) and not BM.

Expanded geometric morphometric analyses of the acanthurid body plan may allow us to assess if head, body, and/or fin shapes are associated with dietary guilds. Additionally, accurately accounting for phylogenetic covariation among shapes will determine which morphological structures are correlated with one another across the phylogeny in a system in which selection may be occurring. Thus, the central aims of this study are to 1) revise the phylogenetic relationships among acanthurids, 2) quantify and describe morphological patterns across surgeonfishes, and 3) explore ecological associations and evolutionary covariation related to morphological subsets within the family using novel phylogenetic comparative methods.

2. Methods

2.1 DNA sequences

DNA sequence data for 125 fish species were analyzed, including 80 species of surgeonfishes and 45 outgroup taxa from several closely related fish families (Appendix A). Tissues and/or data for only 3 extant species of *Acanthurus* were unavailable: *Acanthurus albipectoralis*, *A. chronixis*, *A. fowleri*. The total count of 83 surgeonfishes used here differs from the FishBase.org list of 84 taxa. We reject *A. randalli* and *Prionurus punctatus*; although they remain in FishBase, they are synonyms of *A. bahianus* (Smith-Vaniz et al., 2002) and *P. laticlavius* (Ludt et al., 2019), respectively. We include both *A. nigroris* and *A. nigros* (Randall et al., 2011); *A. nigros* is widespread throughout the Pacific but is not yet listed by FishBase. Portions of 19 genes were analyzed, including eight mitochondrial regions (12S, 16S, ND3, ND4, ND5, ND6, COI, and CYTB) and 11 nuclear markers (ETS2, RAG1, RAG2, TMO4C4,

DLX2, OTX1, BMP4, MYH6, PLAGL2, ZIC1, and RHOD). Many of the data analyzed here were obtained from previous studies (Sorenson et al., 2013; Ludt et al., 2015; Holcroft & Wiley, 2008; Clements et al., 2003; Near et al., 2013; Klanten et al., 2002; Fessler & Westneat, 2007, Appendix A), but we contribute a large set of new DNA sequences for several genes for both acanthurids and outgroups (see Supplementary Methods).

2.2 Time-calibrated phylogenetic analysis and divergence time estimation

Sequences for each gene and the partition model were imported into IQ-TREE 2 (Kalyaanamoorthy et al., 2017; Minh et al., 2020) to construct a maximum likelihood tree, which was then imported into Mesquite (Maddison & Maddison, 2025) for processing to serve as the starting tree in BEAUti 2.7.7. along with the resulting models for nucleotide evolution for each partition (Table S1) obtained from IQ-TREE (details in Supplementary Methods). Based on the best fit partitioning scheme inferred from our IQ-TREE search, we specified separate substitution model parameters for each gene (Table S1). To obtain a time-calibrated phylogenetic hypothesis of Acanthuridae, we estimated divergence times using an optimised relaxed clock (ORC) model and used a standard birth death rate model as a tree prior in BEAST 2.7.7 (Bouckaert et al., 2019; Drummond et al., 2002, 2006). We also used two fossil calibrations for the ORC model. The Middle Eocene *Sorbinithurus sorbinii* from Monte Bolca (Italy), which was identified by Tyler (2000) as a stem member of the Nasinae, was used to assign a minimum age of 48.5 Ma (Papazzoni and Trevisani, 2006) to the crown Acanthuridae. For dating the split of acanthurids from luvarids, we used the Eocene fossil *Kushlukia permira* from the Ypresian (Lower Eocene), identified by Bannikov and Tyler (1995) as a stem luvarid, with a minimum age of 55.8 Ma. For the overall age of acanthurids plus their eupercarian outgroups we set a

minimum age at 100.1 Ma, an average of the estimated ages from recent phylogenomic higher-level studies (Betancour et al. 2017, Near and Thacker 2024, Hughes et al. 2018). Priors for the ORC and standard birth death rate models as well as node ages are outlined in the Supplementary Methods. We ran two independent analyses for 200 million generations, sampling every 5000 generations. Convergence between the two runs was determined based on the appearance of the traces and the degree of trace overlap. Effective sample sizes (ESSs) of all model parameters were used to ensure sufficient independent samples after convergence was reached. All measures were calculated and/or visualized using Tracer v.1.7.2 (Rambaut et al., 2018). A single time calibrated tree was generated from the posterior distribution of trees (first 50% removed as burn-in) using LogCombiner 2.6.3 to combine the trees. Subsequently, TreeAnnotator 2.6.3 (Drummond and Rambaut, 2007) was used to produce the maximum clade credibility tree annotated with mean/median branch lengths and to calculate posterior probabilities for node support.

2.3 Geometric Morphometrics

To investigate the variation in shape across acanthurids, we quantified head, body, and fin morphologies using geometric morphometrics. We collected 231 2D lateral specimen photographs from online museum collections, primary literature, commercial aquarium sites, and our photography (Appendix B). We sampled only adult individuals to limit allometric effects on shape changes and ensuring a standard photograph position. These images span 80 different species across the 6 extant genera within Acanthuridae. Using the R (version 4.4.2, R Core Team, 2024) package “StereoMorph” (Olsen & Westneat, 2015), we placed a total of 183 landmarks (34 fixed landmarks and 149 sliding semilandmarks along 11 curves) on each

specimen image (Figure 1), capturing the variation in body, head, and fin shapes. Morphometrics of soft, movable anatomical elements, such as fins, and variable features such as jaw angle, require standardization of position across images to avoid including non-biologically relevant axes of morphological variation into the datasets, such as the orientation of fins or open mouths. To standardize fin and jaw positions, we developed an app called SurgeonShape written in Objective-C (Supplementary Methods; Figure S1; available at github.com/mwestneat) to spread and rotate fins as well as to calculate comparative and functional traits of the surgeonfish body and fins, including fin areas, fin aspect ratios (ARs), elongation ratio, and other traits. Pectoral and caudal fin ARs were calculated for each specimen using the fin landmarks and the generalized equation:

$$AR = \frac{b^2}{A}$$

where b is the maximum span of the respective fin (line b_{pec} and b_{caudal} in Figure 1) and A is the surface area of the respective fin (curves 5-8 for the pectoral fin and curves and 9-11 for the caudal fin in Figure 1) (George & Westneat, 2019). A straight line between the proximal ends of curves 9 and 11 was used to "close" the area of the caudal fin. Species-average fin ARs were then calculated. Elongation ratio was also calculated by taking the total length of the fish and dividing it by body depth, computed as the vertical distance between the highest point on the body at the center of the dorsal fin and the lowest body point at the origin of the pelvic fin.

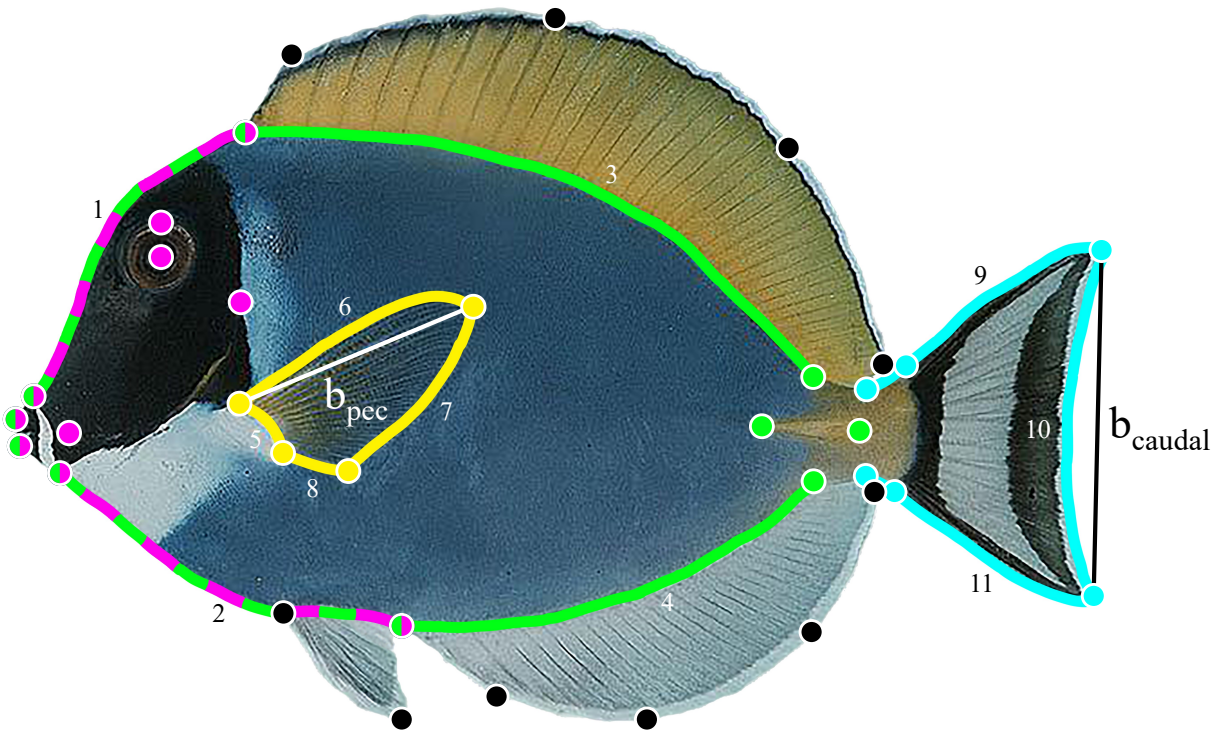

Figure 1. **Geometric morphometric landmark scheme.** Circles represent fixed landmarks, while numbered curves represent sliding semilandmarks. Circles and curves are color-coded based on which landmark subset they belong to: pink denotes head, green denotes body, yellow denotes pectoral fin, and blue denotes caudal fin. Black circles denote landmarks that are not found in any subset but are included in the overall shape of the fish. Lines b_{pec} and b_{caudal} represent the span of the pectoral and caudal fin used in the respective fin AR calculations.

The leveled, rotated, and standardized landmarks were then imported back into R and subsequently divided into multiple subsets (Figure 1): body shape (15 fixed landmarks and 60 sliding semilandmarks along 4 curves), head shape (11 fixed landmarks and 38 sliding semilandmarks along 2 curve), pectoral fin shape (4 fixed landmarks and 28 sliding semilandmarks along 4 curves), and caudal fin shape (6 fixed landmarks and 61 sliding semilandmarks along 3 curves). We elected to use a large number of semilandmarks to aid in the sliding process downstream as increased numbers of semilandmarks help retain the true biological shape of the structure during data analyses. Many of these semilandmarks were removed before final analyses, so that these "helper points" would not prevent us from achieving

appropriate statistical power or drown out shape variation from fixed landmarks (details in Supplementary Materials; Zelditch et al., 2012).

For each landmark subset, we grouped digitized landmarks by species, and then iteratively projected them into linear tangent space by performing a generalized Procrustes analysis (GPA) using the "gpagen" function in "geomorph" (Adams et al., 2025; Baken et al., 2021) to remove any non-shape differences in landmark position attributed to differences in rotation, translation, and scaling. Semilandmarks were slid using the method that reduces bending energy. We calculated species mean shapes using the "mshape" function in "geomorph" (Adams et al., 2025; Baken et al., 2021) and then performed a second GPA, optimizing semilandmark positions by reducing bending energy to project the Procrustes-aligned shape data into linear tangent space using the "gpagen" function in "geomorph" (Adams et al., 2025; Baken et al., 2021) for each subset. We down-sampled the semilandmarks from each landmark subset by deleting the helper points outlined in Supplementary Methods and then performed a principal components analysis (PCA) using the "gm.prcomp" function in "geomorph" (Adams et al., 2025; Baken et al., 2021) to visualize the distribution of taxa in the morphospace across all subsets. For each subset, we projected the time-calibrated phylogeny onto the morphospace, assuming a Brownian motion (BM) model of evolution for estimation of internal node positions, to assess evolutionary directionality of shape changes across Acanthuridae.

2.4 Dietary ecotype categorization

Surgeonfishes' dietary ecotype was categorized through an extensive literature review (Appendix C). While many previous studies use the planktivore/herbivore dichotomy to bin species, we elected here to categorize surgeonfishes into three ecotypes: benthic

herbivores/detritivores, pelagic planktivores, and omnivores. Species were considered omnivorous if explicitly stated in the literature as being omnivorous, or if their primary diet was accompanied by multiple accounts of feeding on secondary prey types.

2.5 Statistical and phylogenetic analyses

We assessed the relationships between surgeonfish morphology and dietary ecotype by performing a permutations-based phylogenetic Procrustes ANOVA on the Procrustes shape variables using the "procD.pgls" function in "geomorph" (Adams et al., 2025; Baken et al., 2021; Collyer & Adams, 2018, 2024) with model structure of coords ~ diet. We used residual randomization in a permutation procedure (RRPP) and performed 1000 iterations for significance testing. This analysis assumes that phylogenetic covariances among species perfectly explain residual error in the model (Collyer & Adams, 2018, 2024). If invalid, this assumption has been shown to lead to increased variance in parameter estimates, reduced power, and, in some cases, elevated type I error rates in phylogenetic regressions (Monteiroa, 2013; Revell, 2010). Thus, accounting for the correct amount of phylogenetic signal in our data is critical, especially considering it has been shown previously that surgeonfishes' linear morphological traits did not evolve under BM, but under a model with selection towards an optimum (Friedman et al., 2016). To account for the correct amount of phylogenetic signal in a Procrustes ANOVA, we estimated the amount of phylogenetic signal (Pagel's λ) in the residual error of our model using methods outlined in previous studies (Natale & Slater, 2022; Navalón et al., 2019). The maximum likelihood estimate of λ derived from this estimation was then used to rescale the phylogeny using the "rescale" function in the R package "phytools" (Pennell et al.,

2014; Revell, 2024), and this transformed phylogeny was used in our phylogenetic Procrustes ANOVA tests.

Continuous fin and body metrics were also tested to see if they related to each other, as well as diet. We performed a phylogenetic generalized least-squares (PGLS) analysis to determine whether pectoral fin and caudal fin ARs were associated using the "pgls" function in "caper" (Orme et al., 2025). Maximum likelihood was used to optimize λ through this function. Additionally, we used a phylogenetic ANOVA to determine if elongation ratio, as well as pectoral and caudal fin ARs, were associated with diet using the function "phylANOVA" in "phytools" (Pennell et al., 2014; Revell, 2024). Here, we accounted for the correct amount of phylogenetic signal in our continuous fin and body metrics using the "phylosig" function in "phytools" (Pennell et al., 2014; Revell, 2024) and then transformed our phylogeny for analysis as described above in our phylogenetic Procrustes ANOVA methods. We conducted post hoc tests to compare the mean among groups and used a Holm-Bonferroni correction to account for multiple testing.

To evaluate the evolutionary covariation between morphological subsets, we performed two-block partial least-squares (PLS) tests using the "phylo.integration" function in the R package "geomorph" (Adams et al., 2025; Baken et al., 2021; Collyer & Adams, 2018, 2024). We elected not to test associations between head and body subsets, as many of their landmarks are shared. Because we are strictly interested in shape covariation between individual blocks, and not their covariation in the context of the whole system, we treated each morphological dataset as a separate block, which does not consider any covariation between subsets due to the variation in their relative size, position, or orientation on the body of the fish.

Importantly, we developed a novel method to accurately account for phylogenetic

covariation among our separate blocks. While “phylo.integration” does account for phylogeny, like “procD.pgls”, it assumes a Brownian motion model of evolution and thus that residual error in the model is perfectly explained by the phylogenetic covariances among species. Here, it is once more imperative to correct for the appropriate amount of phylogenetic signal to avoid incorrect statistical conclusions (Monteiroa, 2013; Revell, 2010). No other study has corrected for the appropriate amount of phylogenetic signal in two-block PLS tests, so here we present a novel method to perform this test. With each two-block PLS comparison of shapes, we estimated the true amount of phylogenetic signal by defining a grid of possible λ values (0 to 1, with increments of 0.01), transforming the phylogeny with the corresponding λ value using the “rescale” function in the R package “phytools” (Pennell et al., 2014; Revell, 2024), and then performing two-block PLS tests with “phylo.integration” in “geomorph” (Adams et al., 2025; Baken et al., 2021) using the transformed phylogeny. For each value of λ, we then computed the multivariate normal likelihood of the resulting PLS scores, assuming an evolutionary covariance matrix where the diagonal elements are the evolutionary rates along each PLS axis, and the off-diagonals are the evolutionary covariances. Importantly, r-PLS, the evolutionary correlation between the two blocks, can be obtained directly from this matrix as:

$$\mathrm{rPLS} = \frac{\mathrm{cov(PLS)}}{\sqrt{rate\ PLS\ X1 * rate\ PLS\ Y1}}$$

where cov(PLS) is the evolutionary covariation between the two PLS axis and rate PLS X1 and rate PLS Y1 are the evolutionary rates of the first PLS axes for first and second block respectively.

We finally chose the λ value that maximized the likelihood of the data (PLS scores) and used this value to rescale our phylogeny as described above for a final two-block PLS test. For those that were found to be significant, the function “compare.pls” in “geomorph” (Adams et al.,

2025; Baken et al., 2021) was used to determine which shapes, if any, are more correlated with one another. PLS correlation coefficients (r-PLS) informed this comparison as well. Additionally, we took the ratio of evolutionary rates along the PLS axes (largest:smallest) to determine how similar the evolutionary rates related to each block were for each comparison.

3. Results

3.1 Acanthurid phylogenetics and time-calibrated tree

The topologies of phylogenetic trees resolved under maximum likelihood (Figure S2) and the time-calibrated topology using Beast (Figure 2) were nearly identical. Estimated ages and posterior probability support for all nodes in the tree, including outgroups, are presented in Figures S3 and S4 respectively. The root node of a monophyletic Acanthuridae was resolved with high support, estimated to be about 54.5 Ma in our phylogenetic chronogram (Figure 2), and all but 11 internal nodes within the phylogeny have unambiguous support. Our phylogenetic tree resolves the genus *Naso* as a strongly supported monophyletic group, with its basal divergence at 19.5 Ma, forming the sister group to all other acanthurids. The genus *Prionurus* was also resolved as a monophyletic group with strong support. It was the second group to branch from the backbone topology of the Acanthuridae, approximately 47 Ma, with a crown age of about 16 Ma. The rest of the acanthurids are split into two clades with strong support at 43 Ma, one containing the monotypic genus *Paracanthurus* and genus *Zebrasoma*, and the other containing the genera *Acanthurus* and *Ctenochaetus*. More detailed phylogenetics results can be found in Supplementary Results.

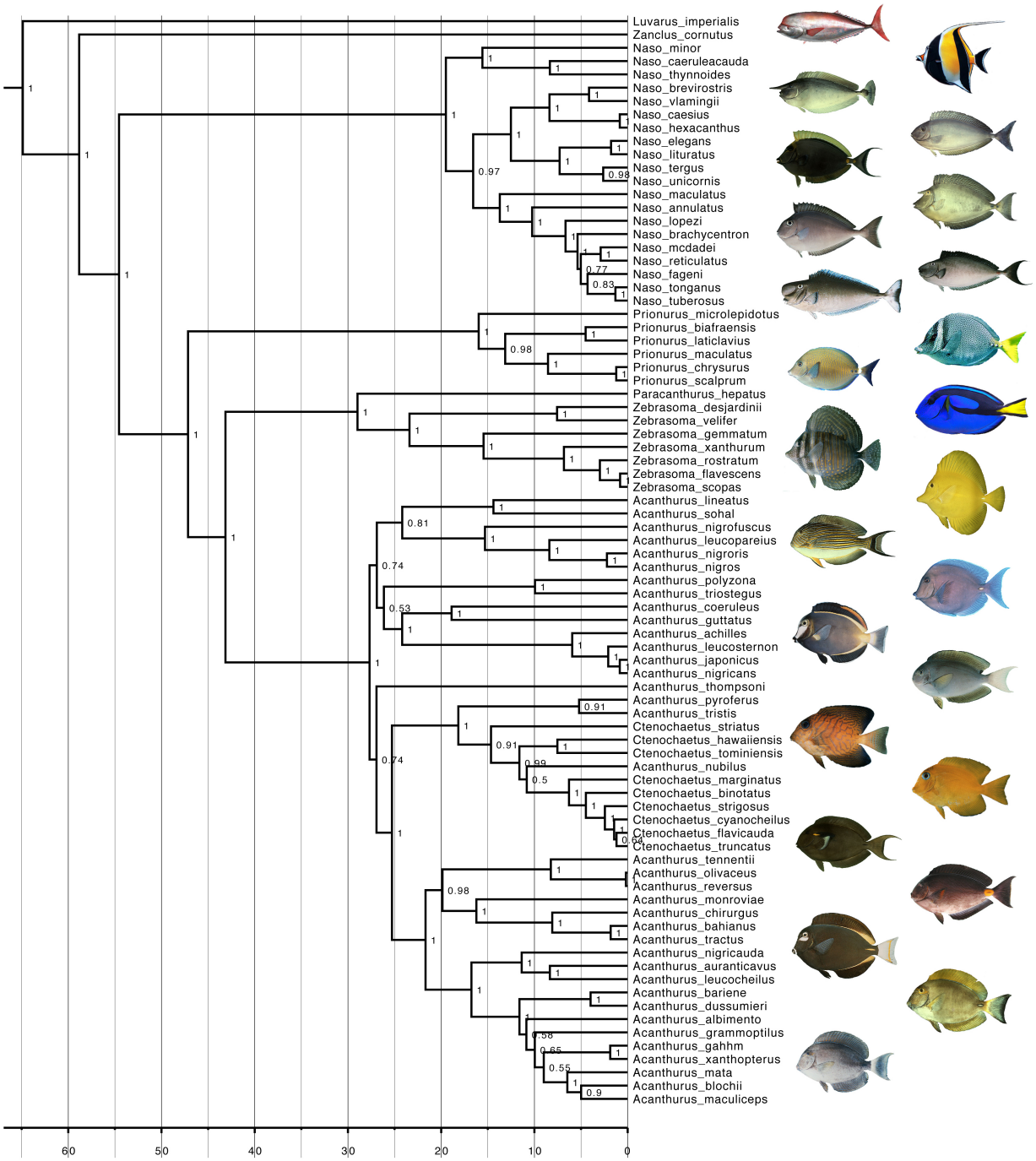

Figure 2. **Phylogenetic Tree.** Time-calibrated phylogenetic hypothesis for the surgeonfishes, family Acanthuridae, including 80 of 83 surgeonfish species as well as outgroups (*Zanclus cornutus* and *Luvarus imperialis*) from related families. Node numbers are support levels computed as the frequency of occurrence of that node in the post burn-in tree set. Only values above 0.9 represent significant support for that node. Supplementary materials (Figures S2-S4) provide additional phylogenetic information.

3.2 Elongation and fin aspect ratios across the phylogeny

Elongation ratios vary across surgeonfishes with *A. guttatus* exhibiting the lowest value (1.861) and *N. lopezi* exhibiting the highest (3.428) values (Figure S5, Appendix D). The acanthurids also exhibit a wide range of fin ARs with pectoral fin ARs ranging from 1.435 in *N. maculatus* to 3.102 in *A. sohal* and caudal fin ARs ranging from 1.251 in *A. albimento* to 3.878 in *N. thynnoides* (Figure 3, Appendix D). When plotted across the phylogeny, elongation ratios indicated that members of the genus *Naso* generally exhibit high ratios (apart from *N. literatus*, *N. elegans*, and *N. unicornis*) compared to all other acanthurid species (Figure S5).

Overall, caudal and pectoral fin AR are significantly negatively correlated even when accounting for shared evolutionary history ($\lambda = 0.45$, adjusted $R^2 = 0.289$ $p < 0.001$). Caudal fin AR mapped onto the phylogeny indicates that members of the genus *Naso* also generally exhibit high AR caudal fins (except for *N. annulatus* and *N. brevirostris*) compared to the rest of the family (Figure 3). Several other *Acanthurus* species demonstrate moderate to high caudal fin ARs, but especially high caudal ARs were limited to the genus *Naso*. Conversely, when the AR of the pectoral fin was examined, an inverse relationship was revealed; *Naso* species exhibited the lowest pectoral fin ARs (except *N. brevirostris*), with just *Z. velifer* exhibiting a somewhat similar pectoral fin AR. *Ctenochaetus* exhibits an opposite, and less extreme relationship seen in *Naso*, with all species exhibiting lower caudal fin ARs and higher pectoral fin ARs (apart from *C. binotatus*). This reciprocal relationship between caudal and pectoral fin AR was not exclusive to *Naso* and *Ctenochaetus*. For example, *P. hepatus*, *A. lineatus*, *A. sohal*, *A. achilles*, *A. guttatus*, *A. thompsoni*, and *A. mata* all exhibit incredibly low caudal fin ARs but some of the highest pectoral fin ARs. Many taxa that exhibit intermediate values of AR in one fin also exhibit intermediate values of AR in the other. Examples include *Naso brevirostris*, *Pr.*

maculatus, *Pr. chrysurus*, *Z. desjardinii*, *A. leucosternon*, *A. tractus*, *A. nubilus*, *A. monroviae*, *A. leucocheilus*, *A. grammoptilus*, and *A. blochii*. However, some taxa do not follow these trends; *Z. velifer* and *N. annulatus* seem to have both low caudal and pectoral ARs. Although no taxa seem to exhibit both high AR pectoral and caudal fins, *A. nigricauda*, *A. xanthopterus*, and *A. gahhm* have one high AR fin paired with a fin with a moderate AR.

3.3 Overall morphological shape patterns

Over 90% of the variation within the complete morphometric dataset is contained in the first seven PCs, with the first two PCs accounting for 74.51% of the total variation in the dataset. PC 1 (58.94%) describes a shift from taxa with short, deep bodies and caudal peduncles, flat foreheads with no apex, short caudal fin ends, pointed, wing-like pectoral fins, deep dorsal and anal fins, and small caudal spin areas (negative scores) to taxa with anteriorly peaked concave foreheads, elongated bodies with narrow caudal peduncles, caudal fins with long trailing edges, round, paddle-like pectoral fins, shallow dorsal and anal fins, and large caudal spin areas (positive scores) (Figure 4). Negative scores on PC2 (15.57%) correspond to taxa with concave foreheads with no apex, extremely convex caudal fins with long training edges, and pointed pectoral fins with positive scores correspond to taxa with flat foreheads, concave caudal fins, and rounder pectoral fins. These differences described by the first two PC axes almost completely separates genera into distinct regions of morphospace. No statistics related to associations with variables of interest were done on our full shape data, as the number of variables (146, stemming from the x and y coordinates of our 73 landmarks) exceeded our number of individuals (80 average species shapes). Phylomorphospaces were generated for all four subsets (caudal fin, pectoral fin, head, and body), pruning our data to include only taxa in the tree as well as to

exclude outliers for each subset, and appropriate associations were investigated.

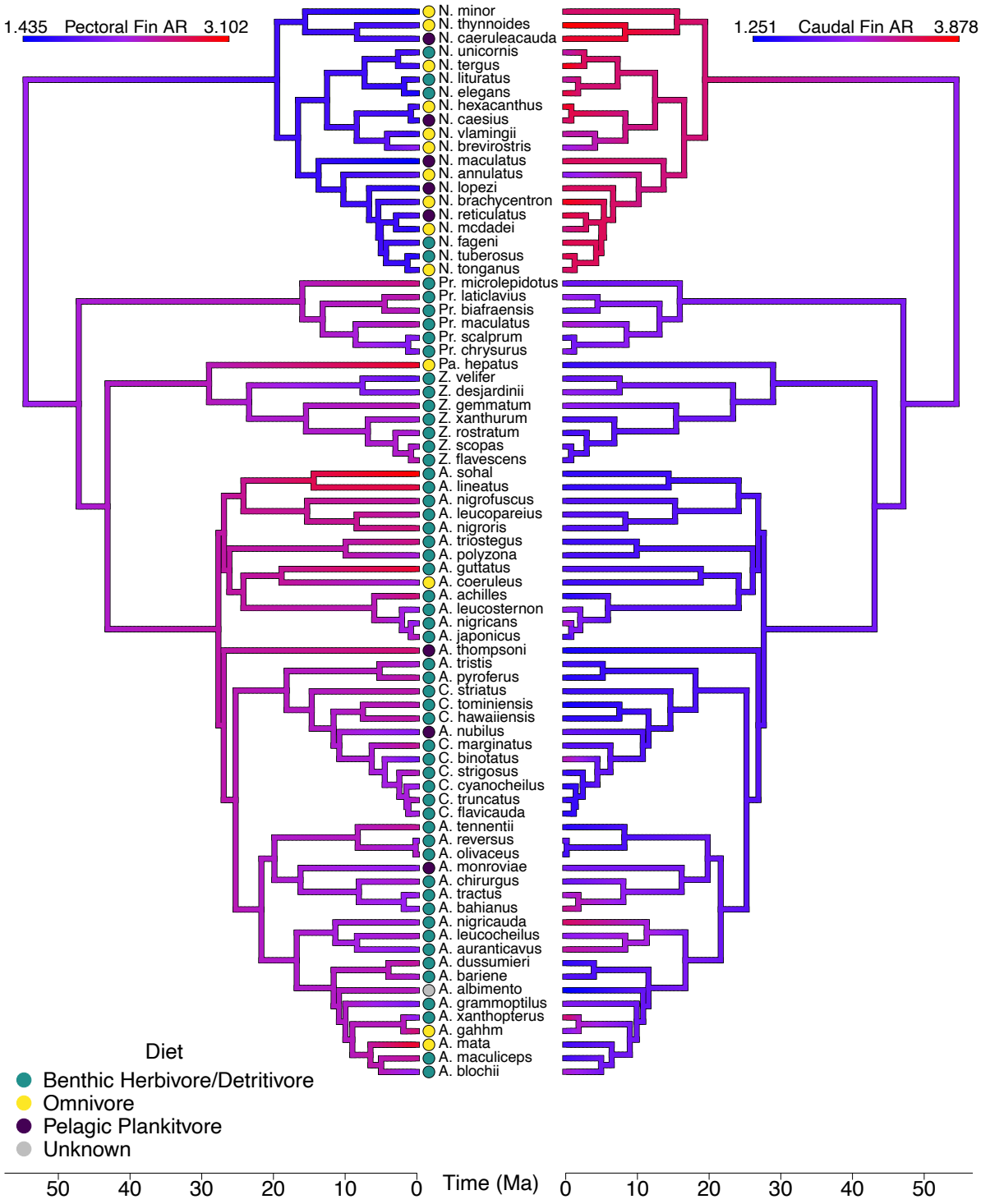

Figure 3. **Fin Aspect Ratio Mirror Trees.** Caudal and pectoral fin ARs mapped along the Acanthuridae phylogeny by estimating states at internal nodes using maximum likelihood, with

caudal fin AR ranging from 1.251 to 3.878 and pectoral fin AR ranging from 1.435 to 3.102. Length is measured in Ma, and time is also denoted on the bottom scale. High/low caudal fin AR is generally associated with low/high pectoral fin AR, respectively, across the phylogeny. Dietary ecotype for each species is represented by colored dots at the tips of trees.

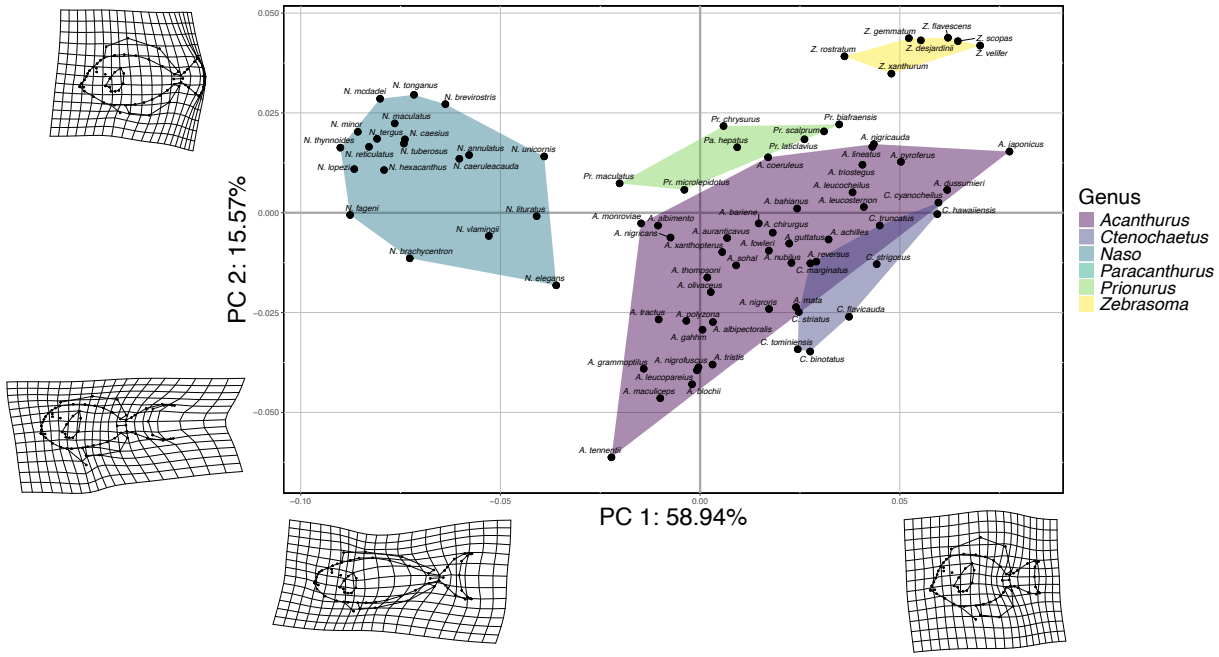

Figure 4. **Full Shape Morphospace.** PCA plot showing PC 1 (58.94%) vs PC 2 (15.57%) of the 79 shapes representing the mean shape of each species present in the dataset. Genera are indicated by convex hulls. Thin plate splines of the minimum and maximum values of each PC are shown at the corresponding ends of each axis as a deformation of the mean shape of all specimens.

3.4 Patterns and associations across phylomorphospaces

The first two PCs account for 69.69% of the total variation within our pectoral fin shape dataset, with over 90% being accounted for in the first 5 PCs. Negative PC 1 (47.19%) scores correspond to taxa with thin, elongated, high AR pectoral fins and positive scores of PC1 correspond to taxa with stout, short, low AR pectoral fins (Figures 5 & S6). PC 2 (22.50%) visualizes a shift from taxa with round pectoral fins with short trailing edges (negative scores) to taxa with sharp pectoral fins with longer trailing edges. *Naso* species exclusively occupy positive PC 1 scores corresponding to low pectoral fin ARs (Figure S6). However, *N. brevirostris* appears

to be converging on *Zebrasoma* species in the lower left quadrant (-PC1, -PC2) corresponding to higher pectoral fin AR. Variation in caudal fin AR seems to be strongly associated with shape variation along PC1, visually corroborating the significant negative correlation between pectoral and caudal fin AR (Figures 5 & S6).

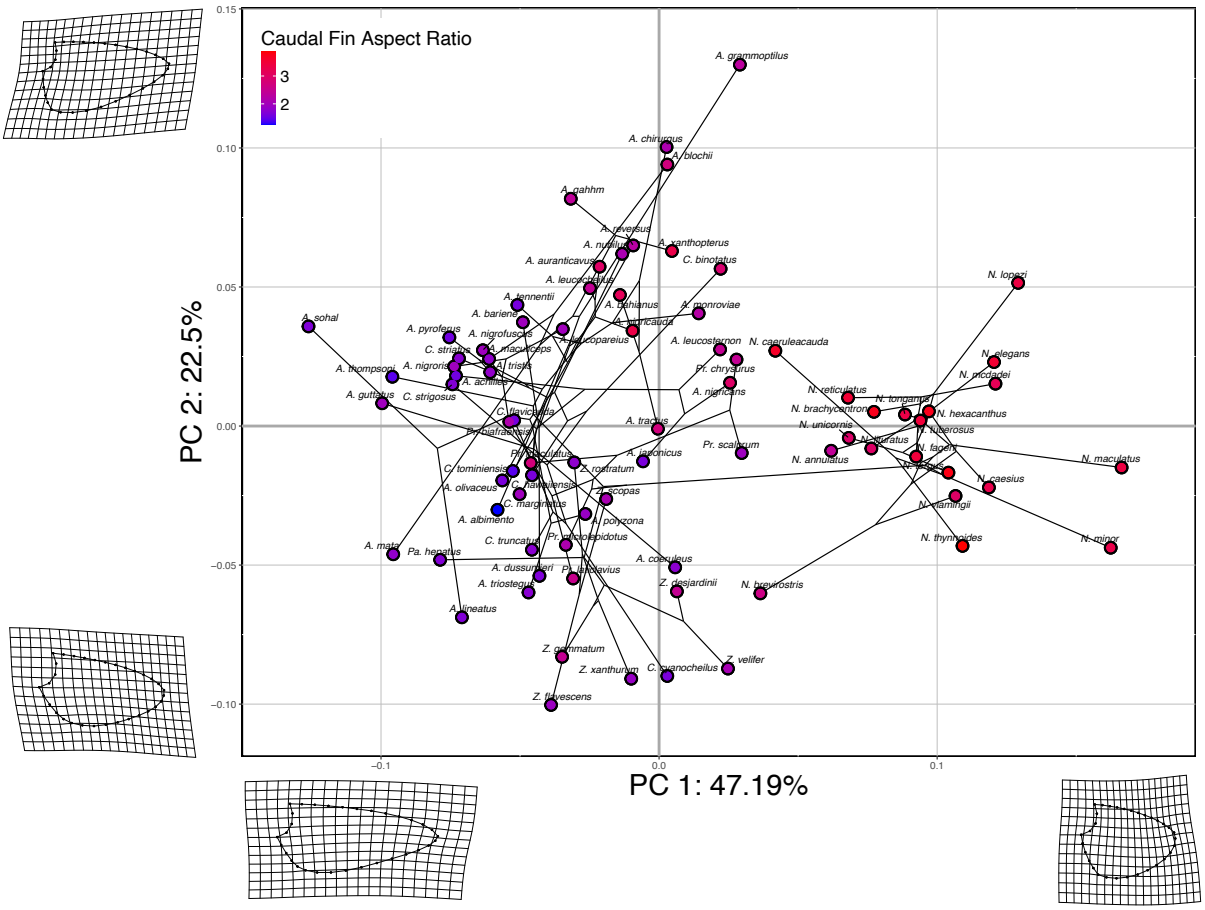

Figure 5. **Pectoral Fin Phylomorphospace.** PCA plot showing PC 1 (47.19%) vs PC 2 (22.5 %) of the 79 shapes representing the mean pectoral fin shape of each species present in the dataset. Points are color-coded on a gradient of caudal fin AR. Cooler colors represent lower values of caudal fin AR, whereas warmer colors represent higher values. Thin plate splines of the minimum and maximum values of each PC are shown at the corresponding ends of each axis as a deformation of the mean shape of all specimens.

Our caudal fin phylomorphospace also shows a significant negative correlation between pectoral and caudal fin AR. Over 90% of the variation is captured in the first three PCs, with the

first two containing 86.45% of the overall variation in our data. PC 1 (66.25%) describes a shift from taxa with very convex caudal fins with long trailing ends, curved dorsal and ventral sides, and a wide base (negative scores), to taxa with concave caudal fins with no exaggerated trailing ends, straight dorsal and ventral sides, and a narrow base (positive scores) (Figures 6 & S7). Negative scores on PC 2 (20.2%) correspond to slightly convex caudal fins with a wide base, but no sharp, exaggerated trailing ends, while positive scores correspond to taxa with very convex caudal fins with long trailing ends and sharp fin tips, similar to negative PC1 scores, but with a much narrower base. *Acanthurus* and *Ctenochaetus* overlap extensively, as in our pectoral fin phylomorphospace, but *Prionurus* now only overlaps with *Acanthurus* species. *Pa. hepatus* and *A. polyzona* converge on negative PC 2 values. *Naso* species cluster with positive PC 2 scores while *Zebrasoma* species cluster in the lower right quadrant (+PC1, -PC2). *Naso* spans the entire PC 1 axes and approaches some *Acanthurus* species' shapes, while *N. brevirostris* converges on fin shapes common in *Zebrasoma* (lower right quadrant) (Figure S7). Variation in pectoral fin AR seems to be more strongly associated with shape variation along PC2, though some variation is also associated with changes along PC1.

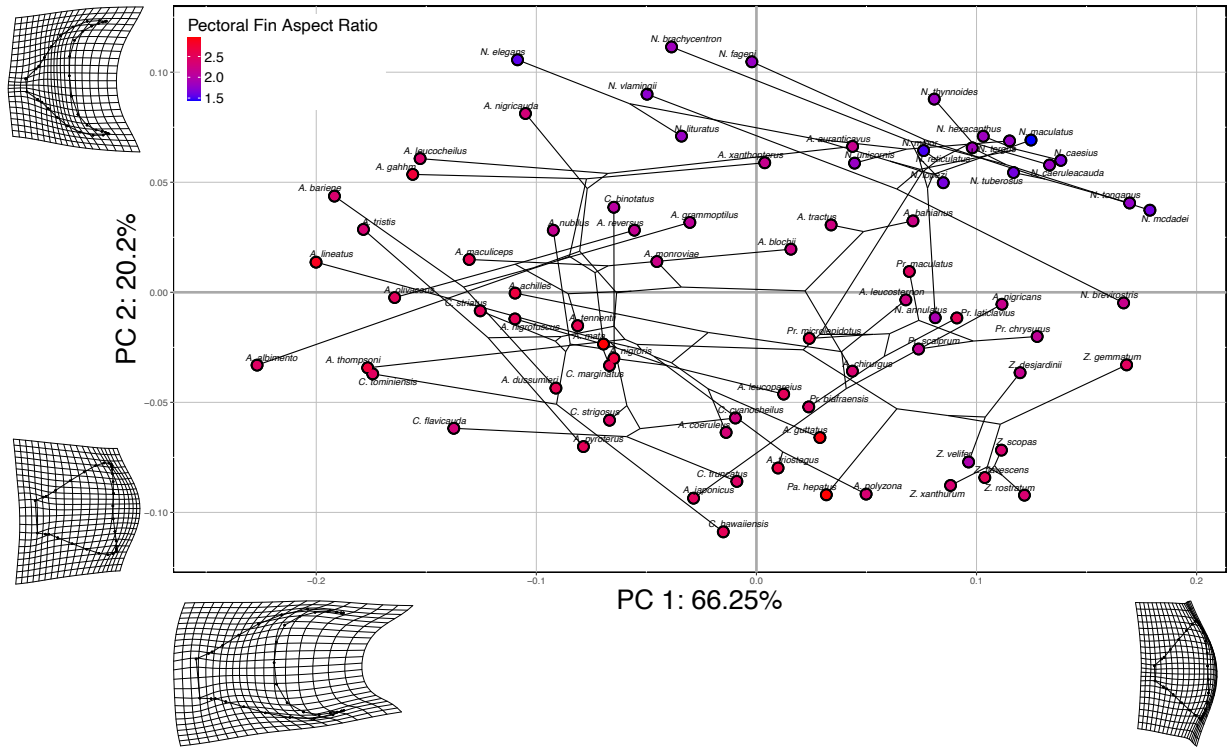

Figure 6. **Caudal Fin Phylomorphospace.** PCA plot showing PC 1 (66.25%) vs PC 2 (20.2%) of 79 shapes representing the mean caudal fin shape of each species present in the dataset, with *A. sohal* removed as it is an outlier. Points are color-coded based on a gradient of pectoral fin AR. Cooler colors represent lower values of pectoral fin AR whereas warmer colors represent higher values. Thin plate splines of the minimum and maximum values of each PC are shown at the corresponding ends of each axis as a deformation of the mean shape of all specimens.

The first two PCs of the head shape phylomorphospace make up 60.42% of the overall variation in our dataset with 90% of the variation captured in the first 7 PCs. Negative scores of PC 1 (42.94%) correspond to taxa with longitudinally compressed, but sagittally expanded heads with straight/convex profiles and a pointed snout while positive PC 1 scores correspond to taxa with longitudinally expanded, but sagittally compressed heads with concave profiles and a rounded snout (Figures 7 & S8). PC 2 (17.48%) corresponds to a shift in taxa with anterior placed eyes, straight foreheads, and small mouths (negative scores) to taxa with posteriorly placed eyes, exaggerated, concave foreheads, and a large mouth (positive scores). *Zebrasoma* species converge on *Ctenochaetus* and *Acanthurus*, while *Prionurus* has diverged from this

group with three *Acanthurus* species: *A. thompsoni*, *A. mata*, and *A. nubilus*. *Zebrasoma rostratum* and *Pa. hepatus* cluster with many *Naso* species (+PC 1, +PC 2) while three *Naso* species (*N. elegans*, *N. literatus*, and *N. unicornis*) cluster with *Ctenochaetus* species (-PC 1, slightly +PC 2). Dietary ecotype is visually associated with shape variation along PC 1 with benthic herbivores/detritivores found in negative PC 1 space and omnivores and pelagic planktivores found in positive PC 1 space. The three divergent *Acanthurus* species (towards + PC 1) are all either omnivorous or planktivorous unlike the majority herbivorous/detritivorous *Acanthurus* species, and the three divergent *Naso* species (towards -PC 1) are all herbivorous/detritivorous, unlike the majority omnivorous or planktivorous *Naso* species.

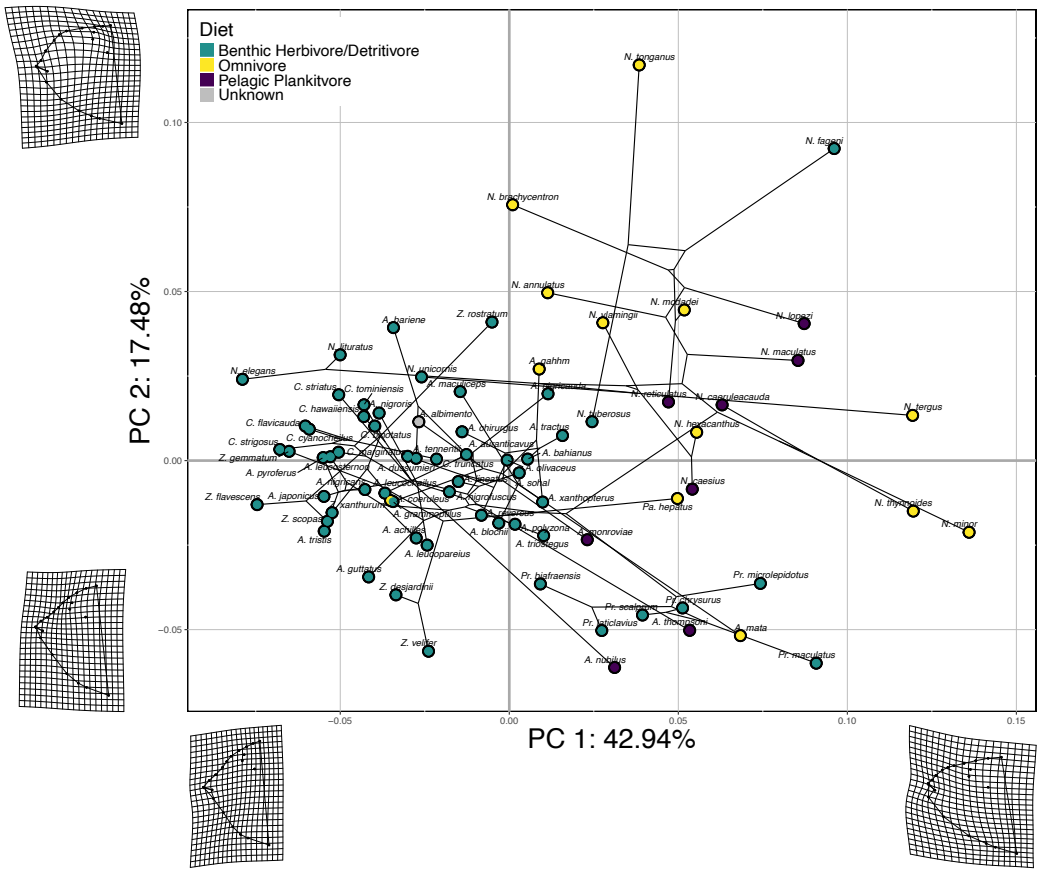

Figure 7. **Head Shape Phylomorphospace.** PCA plot showing PC 1 (42.94%) vs PC 2 (17.48%)

of 79 shapes representing the mean head shape of each species present in the dataset, with *N. brevirostris* removed as it is an outlier. Points are color-coded based on dietary ecotype. Thin plate splines of the minimum and maximum values of each PC are shown at the corresponding ends of each axis as a deformation of the mean shape of all specimens.

Over 90% of the variation in the body shape dataset is contained in the first four PCs, with 83.85% of the overall variation captured by PC 1 and PC 2. PC 1 (77.62%) corresponds to a shift in taxa with stout, rounded bodies with wide caudal peduncles and shorter caudal spine areas (negative scores) to taxa with elongated bodies with narrow caudal peduncles and longer caudal spine areas (positive scores) (Figure 8). Negative PC 2 (6.23%) scores represent taxa with square, convex head profiles and shorter caudal spine areas while positive PC 2 scores represents taxa with concave, round head profiles and longer caudal spine area. *Naso* species cluster with positive PC 1 values while *Zebrasoma* species cluster in the lower left quadrant (-PC 1, -PC 2). *Ctenochaetus* and *Acanthurus* species (-PC 1) overlap with *Prionurus* species (-PC 1, +PC 2) along PC 1. Dietary ecotype is visually associated with shape variation along PC 1, but not as strong as seen in our head shape results. While benthic herbivores/detritivores are mostly found in negative PC 1 space, the five benthic herbivores/detritivores *Naso* species are found at more positive PC 1 values with omnivores and pelagic planktivores.

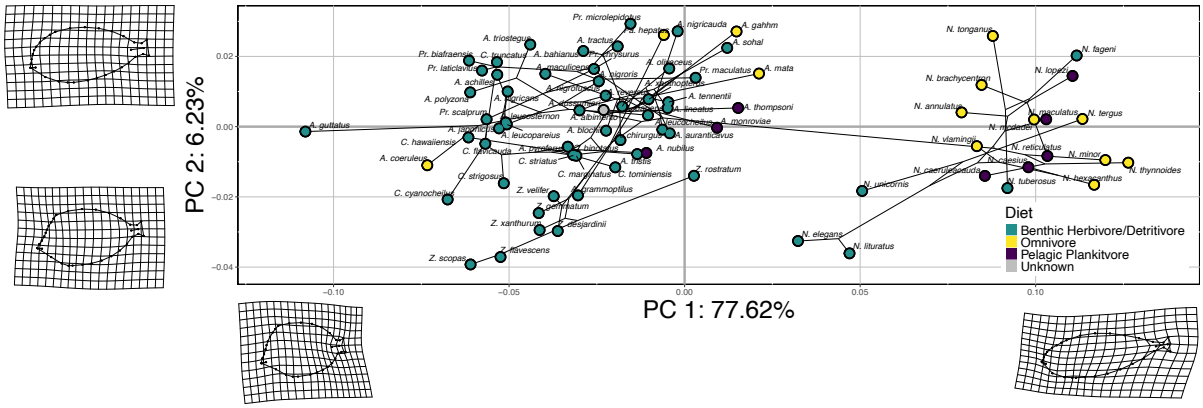

Figure 8. **Body Shape Phylomorphospace.** PCA plot showing PC 1 (77.62%) vs PC 2 (6.23%)

of 79 shapes representing the mean head shape of each species present in the dataset, with *N. brevirostris* removed as it is an outlier. Points are color-coded based on dietary ecotype. Thin plate splines of the minimum and maximum values of each PC are shown at the corresponding ends of each axis as a deformation of the mean shape of all specimens.

3.4 Ecomorphology associations

A significant association between both head and body shape variation with dietary ecotype was found, but no significant associations were found between diet and our fin shape datasets (Table 1). Similarly, while no significant associations were found between diet and both pectoral fin and caudal fin ARs, a significant association exists between diet and elongation ratio (Table 2). When looking at pairwise tests using the Holm-Bonferroni correction, benthic herbivores/detritivores significantly differed from both omnivores ($p < 0.01$) and pelagic planktivores ($p < 0.01$) in elongation ratio while pelagic planktivores and omnivores did not significantly differ.

Table 1. **Phylogenetic ANOVA Results for Shape**. Summary of the results from each phylogenetic ANOVA testing whether morphological subsets are related to diet. The sums of squares (SS), mean squares (MS), R-squared value, F statistic, Z statistic, and p-value are reported for each term. For each term, df = 2. Statistics for the model residuals and the totals can be found in Supplementary Materials. Statistically significant relationships between shape and diet were based on 1000 iterations for significance testing. ($p < 0.001$ = ***)

	SS	MS	R^2	F	Z	p-value
Pectoral Fin Shape	0.0004622	0.00023110	0.03932	1.5348	1.1457	0.123
Caudal Fin Shape	0.0001285	0.000064244	0.00683	0.2544	-1.9567	0.977
Head Shape	0.0012208	0.00061041	0.14817	6.4359	4.4458	0.001 ***
Body Shape	0.0005219	0.00026095	0.13062	5.5593	3.4024	0.001 ***

Table 2. **Phylogenetic ANOVA Results for Continuous Metrics**. Summary of the results from each phylogenetic ANOVA testing whether continuous fin and body metrics are related to diet. The sums of squares (SS), mean squares (MS), F statistic, and p-value are reported for each term. For each term, df = 2. Statistics for the model residuals can be found in Supplementary Materials. Statistically significant relationships between shape and diet were based on 1000 iterations for significance testing. ($p < 0.001$ = ***)

	SS	MS	F	p-value
Pectoral Fin AR	1.776391	0.888196	7.438682	0.131
Caudal Fin AR	7.042684	3.521342	8.555661	0.071
Elongation Ratio	5.138866	2.569433	36.902012	0.001 ***

3.5 Strength of morphometric correlations and evolutionary rates along PLS axes

We used a novel two-block PLS tests to quantify the evolutionary correlations between our morphological subsets and rates of evolution within them while simultaneously estimating phylogenetic signal (Table 3). PLS correlation coefficients ranged from 0.356 (pectoral fin shape vs head shape) to 0.61 (caudal fin shape vs body shape), suggesting weak to moderately strong evolutionary correlations between shapes. Only two of these associations were found to be significant after correcting for multiple comparison: caudal fin shape vs body shape ($Z = 3.480$, uncorrected p-value < 0.001, corrected p-value < 0.01, r-PLS = 0.61, Figure 9) and caudal fin shape vs pectoral fin shape ($Z = 3.995$, uncorrected p-value < 0.001, corrected p-value < 0.01, r-PLS = 0.591, Figure 10). The evolutionary correlation strength was not significantly different between these two analyses. No other tested shape pairs exceeded the significance level with the Holm-Bonferroni correction, although caudal fin shape vs head shape was significant before the correction. At the extremes, PLS axes exhibit nearly identical evolutionary rates (σ ratio between pectoral fin and head shape = 1.087) to rates of evolution almost five times greater in one PLS axis than the other (σ ratio between caudal fin and head shape = 4.924), while the significant correlations of caudal fin shape and pectoral fin shape, as well as caudal fin shape and body shape, exhibited σ ratios of 2.444 and 1.484, respectively.

Table 3. **Two-Block PLS Results**. Summary of the results from each two-block PLS test done on each morphological subset pairing (except head shape vs body shape). Raw p-values and Bonferroni-corrected p-values are stated, along with the PLS correlation coefficients (r-PLS) and

effect sizes (Z) for each comparison. The λ value that maximized the likelihood of the data (PLS scores) used to rescale the phylogeny is reported, along with its corresponding log likelihood and AIC scores. The evolutionary rates along PLS axes are noted (PLS σ) as well as their ratio. ($p < 0.01$ = **, $p < 0.05$ = *)

Block 1 Shape	Block 2 Shape	p-value (raw)	p-value (corrected)	r-PLS	Effect Size (Z)	λ	logLik	AIC	PLS1 σ	PLS2 σ	σ ratio
Caudal	Pectoral	0.001**	0.005**	0.591	3.9949	0.21	544	-1083	9.63E-05	3.94E-05	2.444
Caudal	Head	0.043*	0.215	0.391	1.6709	0.2	538	-1071	1.30E-04	2.64E-05	4.924
Pectoral	Head	0.348	1	0.356	0.4093	0.24	583	-1160	3.37E-05	3.10E-05	1.087
Caudal	Body	0.001**	0.005**	0.61	3.4795	0.16	593	-1181	4.05E-05	2.73E-05	1.484
Pectoral	Body	0.06	0.3	0.376	1.5544	0.35	593	-1179	4.09E-05	2.02E-05	2.025

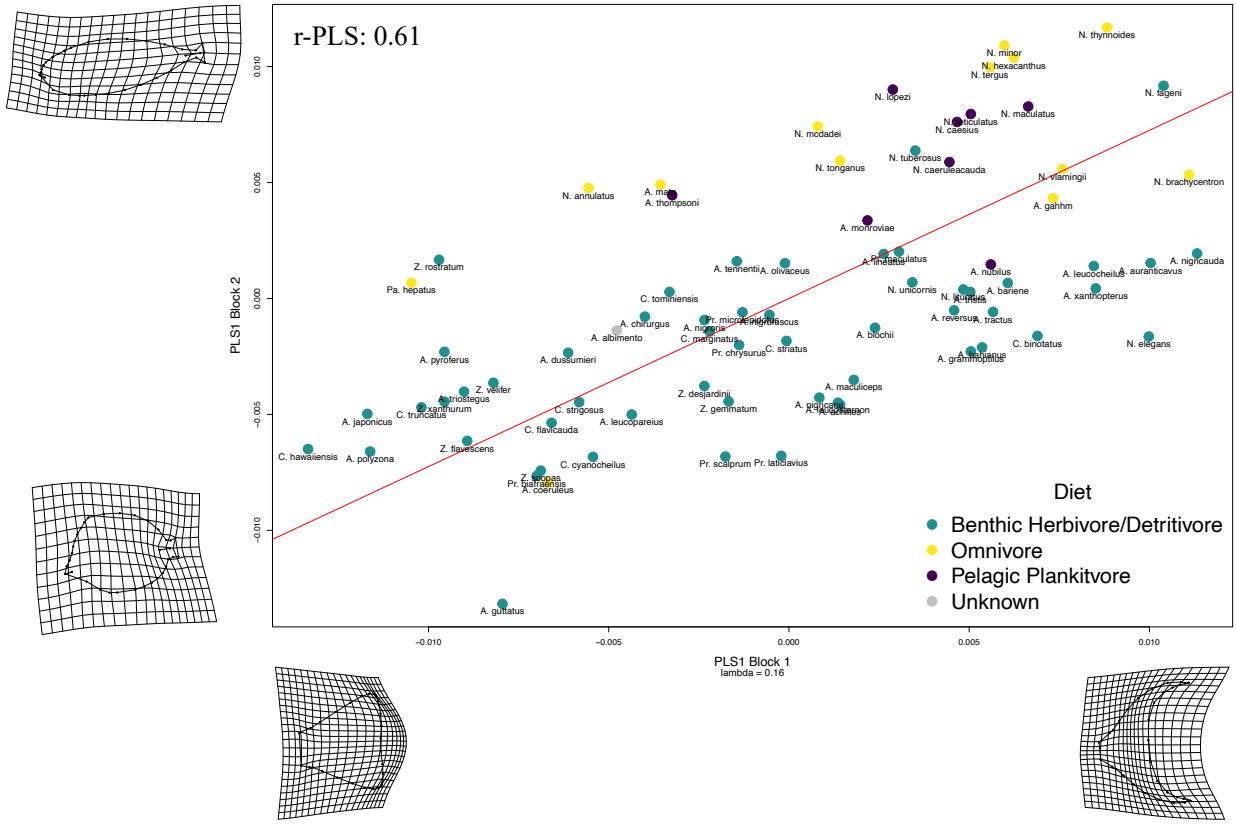

Figure 9. **Caudal Fin Shape vs Body Shape Two-block PLS.** Plots showing the first PLS scores for caudal fin shape (block 1) and body shape (block 2). Caudal fin shape and body shape are significantly paired (p-value < 0.01), with a PLS correlation coefficient of 0.61. The red line indicates the correlation between the two PLS axes yielded by a phylogenetically-informed PLS test. The lambda value used to rescale the tree for analysis is denoted below the PLS1 Block 1

axis. Thin plate splines at the axes' extremes visualize shape change across their respective axes. Points are color-coded based on dietary ecotype.

4. Discussion

Development of well-resolved and species-rich phylogenies for diverse fish groups, in combination with detailed morphometric and ecological data sets, can yield new insights into the evolutionary history of anatomical and functional diversification. Here, we robustly analyze shape across the surgeonfish body plan and compute important functional traits using geometric morphometrics improved by standardized biomechanical fin rotations. We present a new time-calibrated phylogeny of the Acanthuridae that revises species groupings and serves as a critical backbone for evolutionary analysis. The central conclusions of this study are (1) almost all morphospaces visually supports our molecular phylogenetic groups with the full shape morphospace visually supporting classic taxonomy, (2) surgeonfishes have evolved a strong inverse relationship between caudal fin and pectoral fin shape in which a high/low aspect ratio (AR) caudal fin is paired with a low/high AR pectoral fin, with strong locomotor implications, (3) surgeonfish head and body shapes (independent of the fins) are significantly related to their dietary ecotype, and (4) shared evolutionary history does not fully explain the shape correlations seen in surgeonfishes; these correlations are variable, with caudal fin shape not only significantly covarying with the body and pectoral fin, likely due to ecological and functional demands, respectively, but also exhibiting the highest evolutionary rates among morphometric subsets. Below we detail our insights into surgeonfish phylogeny and ecomorphology using new tools for morphometrics, biomechanics, and comparative methods and discuss the need for more investigation into the relationship between evolutionary rate differences and degree of covariation across shapes.

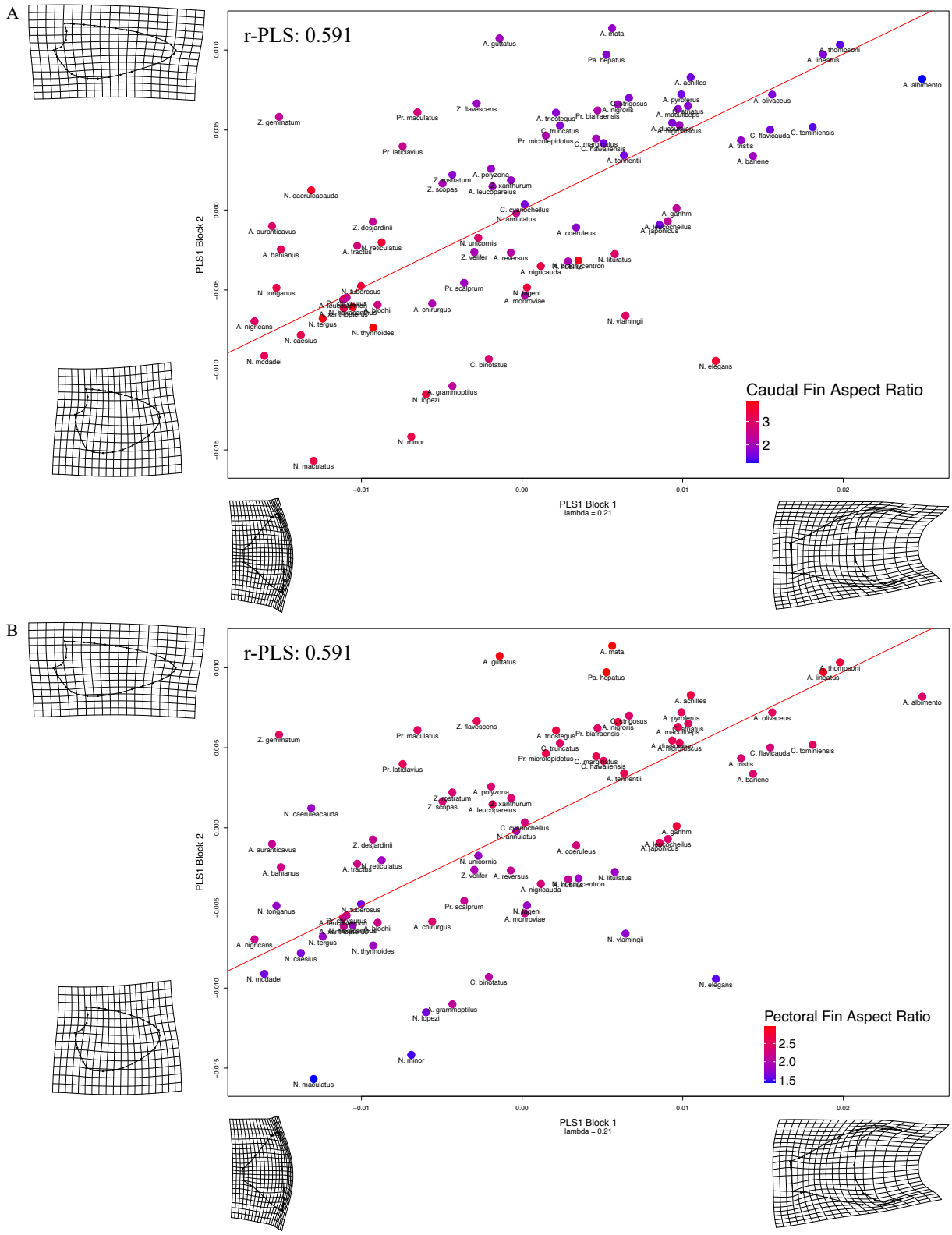

Figure 10. **Caudal Fin Shape vs Pectoral Fin Shape Two-block PLS.** Plots showing the first PLS scores for caudal fin shape (block 1) and pectoral fin shape (block 2). Caudal fin shape and

pectoral fin shape are significantly paired (p-value < 0.01), with a PLS correlation coefficient of 0.591, indicating a moderately strong correlation between shapes. Pectoral fin and caudal fin shape are inversely related: low/high AR pectoral fins are correlated with high/low AR caudal fins. The red line indicates the correlation between the two PLS axes yielded by a phylogenetically-informed PLS test (note the origin is high AR pectoral and low AR caudal). The lambda value used to rescale the tree for analysis is denoted below the PLS1 Block 1 axis. Thin plate splines at the axes' extremes visualize shape change across their respective axes. Points are color-coded on a gradient to indicate mean (A) caudal fin AR and (B) pectoral fin AR for each species. Cooler colors represent lower values of fin ARs, whereas warmer colors represent higher values of fin ARs.

4.1 Morphometric Support for Phylogenetic Relationships of the Acanthuridae

The expanded molecular phylogenetic analysis of surgeonfishes presented here is the most complete in terms of taxonomic sampling and number of loci, encompassing 97% of surgeonfish diversity and adding 10 additional loci. Our new molecular phylogeny confirms many of the relationships previously proposed in several morphological trees (Guiasu & Winterbottom, 1993; Winterbottom, 1993) as well as expands and refines the conclusions made in previous molecular phylogenies (Clements et al., 2003; Klanten et al., 2004; Sorenson et al., 2013), which is discussed in more detail in the Supplement. Our morphometric data provide new insights into the placement of *Acanthurus* and *Ctenochaetus* within the surgeonfish phylogeny.

The distinction between *Acanthurus* and *Ctenochaetus* as separate genera has long been debated in the literature, and the likelihood that *Acanthurus* is paraphyletic with respect to *Ctenochaetus* had previously been suggested (Randall 1955, Winterbottom 1993, Guiasu and Winterbottom 1993) using osteological and meristic characters as well as by Sorenson et al. (2013) using molecular markers. *Acanthurus* and *Ctenochaetus* overlap in morphospace for all morphological subsets (Figures 5-8), though some morphometric differences exist between the two groups. The full shape morphospace (Fig. 4) shows distinctions among genera, with *Ctenochaetus* showing a split from *Acanthurus* species with only slight overlap, visually

agreeing with classic taxonomic groupings. More overlap and shared morphospace are seen in the head (Fig. 7) and body (Fig.8) morphospaces corresponding to heads that are straight and more longitudinally compressed, but sagittally expanded, and a more rounded body. It is intriguing that the full shape data (Figure 4) conflicts with phylogeny, supporting the classic taxonomic classification of *Acanthurus* and *Ctenochaetus*. The recommendation made by Clements et al. (2003), Klanten et al. (2004) and Sorenson et al. (2013) that *Acanthurus* and *Ctenochaetus* should be merged into the single genus *Acanthurus* is supported by our phylogenetics and all our morphometric datasets except our full shape data. The repeated and conclusive combination of molecular phylogenetic and most morphometric data seems sufficient to formally propose this taxonomic change in a future treatment of acanthurid classification.

4.2 Evolution of fin shape related to locomotion of surgeonfishes

Surgeonfishes have evolved two alternative combinations of propulsive fin shape, one with a high AR caudal fin and low AR pectoral fins, and the other with high AR pectoral fins and a low AR caudal fin (Figures 3, 5, 6), with several intermediate AR combinations. *Naso* species have distinct caudal and pectoral fin shapes compared to the rest of the family, with sharp, high AR caudal fins and rounded, low AR pectoral fins. The evolution of a high/low AR tail with low/high AR pectoral fins has biomechanical and locomotor significance, with the former pairing associated with body-caudal fin propulsion and the latter with labriform propulsion. Surgeonfishes are some of the fastest fishes according to field measurements of typical, steady, swimming behaviors in wave-swept reef areas (Fulton et al. 2005; Fulton 2007). These fast speeds are found primarily within *Acanthurus* species employing labriform propulsion, but *Naso* and some other species that primarily oscillate the tail are high-performance swimmers as well,

suggesting the importance of fin shape across all swimming modes.

The main axis of variation in pectoral fin morphology across many fishes is the distinction between high AR, flapping fins that facilitate efficiency and speed during swimming, versus low AR, paddling fins that are specialized for maneuverability (Gerstner, 1999; Walker & Westneat, 2000, 2002), with ARs above about 2.0 usually considered to be wing-shaped, high AR fins (Walker & Westneat, 2000; Westneat et al., 2017). Our fin shape analyses show that *Acanthurus*, *Ctenochaetus*, *Paracanthurus*, *Prionurus*, and *Zebrasoma* tend to have high, wing-like AR pectoral fins well suited for flapping kinematics, whereas members of the genus *Naso* have low AR, paddle-shaped pectoral fins, likely to maneuver effectively. The pelagic lifestyle of *Naso* species could contribute to the need for pectoral fins built for maneuverability. These results suggest that the key biomechanical trend in pectoral fin shape reflecting the thrust efficiency vs maneuverability paradigm found in wrasses and parrotfishes is operating in the surgeonfishes system as well, yet few biomechanical analyses of pectoral fin locomotion have been performed in surgeonfishes (Mihalitsis & Wainwright, 2024; Perevolotsky et al., 2020; Schakmann & Korsmeyer, 2023). Future work on pectoral kinematics integrated with musculoskeletal design and neural control (Drucker, 1996; Flammang & Lauder, 2013; Westneat, 1996) on a range of acanthurids performing steady swimming and maneuvering behaviors may yield important insights into locomotor trade-offs in this group.

A similar, but inverse, relationship is found in surgeonfish caudal fin morphology. The main axis of variation is a spectrum ranging from high AR caudal fins that exhibit a narrowing of the caudal peduncle to low AR caudal fins with wider peduncles. High AR caudal fins have been shown to increase the lift-drag ratio during swimming, allowing for efficiency and greater endurance swimming speeds (Sambilay, 1990), while low AR fins are associated with high-

speed sprint swimming (Weihs, 1973; Webb, 1982). *Naso* species tend to exhibit high caudal fin ARs while the other genera exhibit low caudal fin ARs. The pelagic lifestyle of *Naso* may have led to a specialized caudal fin morphology for high-efficiency body-caudal fin propulsion, although several *Naso* species live in the benthic zone for some of their life history (Klanten et al., 2004, Appendix C). Analysis of various caudal fin morphologies has also revealed that narrower peduncles and some degree of forking (as opposed to no forking, or extreme forking) allow for enhanced propulsive performance (Krishnadas et al., 2018). These distinct caudal fin traits create high ARs and are exhibited by the majority of *Naso* species. Other research has indicated that crescent-shaped caudal fins (another high AR shape) yield less thrust than their less-curved counterparts, but are more efficient when cruising (Chang et al., 2012). It is likely that the caudal fin morphology of *Naso* species is specialized for the unique swimming mode of the unicornfishes, which relies heavily on caudal fin, rather than pectoral fin, propulsion, for enhanced and efficient propulsion while cruising in an open pelagic environment off the reef slope. Exploration of swimming kinematics, axial musculature, and the search for distribution of red muscle and characteristic axial tendons similar to those of mackerels and tunas (Westneat & Wainwright, 2001) may be a productive avenue for future research on high-performance axially swimming surgeonfishes.

Expanding these ideas broadly across the reef fishes could reveal large-scale patterns of caudal and pectoral fin shape evolution. Pectoral fin AR has been measured in 46 species of damselfishes (Pomacentridae) and ranges from 0.63 to 1.67 (Fulton et al. 2005), suggesting these fishes exhibit lower pectoral fin ARs. The family Labridae, with over 600 species, is the only other reef fish family for which pectoral AR measures are fairly comprehensive (Wainwright et al., 2002; Westneat et al., 2017). Labrids have more variation in their pectoral fin ARs than

surgeonfishes and damselfishes; values range from 0.8-4.6 across 340 species with over 150 species exhibiting high AR wing-like fins (AR > 2.0). Adding additional measurements of caudal fin AR and fin shapes to these taxa as well as including more closely related groups to acanthurids like the angelfishes and butterflyfishes would uncover if these fin shape relationships discussed have evolved across reef fishes in general.

4.3 Ecomorphology related to the evolution of head and body shape of surgeonfishes

Combining results from the phylomorphospaces, statistical tests, and thin plate splines, descriptions of significant morphological associations of the head and body related to dietary ecotype are supported. Benthic herbivores/detritivores have a distinct head and body shape from that of omnivores and pelagic planktivores. Benthic herbivores/detritivores tend to have small mouths, straight foreheads with a more longitudinally compressed, but sagittally expanded head, and stout, rounded bodies with a smaller caudal spine area that extends past the caudal peduncle (Figures 7, 8, & S8). Omnivores and pelagic planktivores share similar forms that differ from benthic herbivores/detritivores, both exhibiting larger mouths, rounded heads that are longitudinally expanded, but sagittally compressed with an anterior apex, and more elongated bodies (Figures 7, 8, & S8). Head shape and body elongation have been previously shown to be functionally important to fishes, being associated with habitat, trophic niches, and feeding modes, potentially limiting the range of possible head and body morphologies fishes can exhibit and affecting evolutionary rates (Bejarano et al., 2017; Claverie & Wainwright, 2014; Cooper & Westneat, 2009; Floeter et al., 2018; Friedman et al., 2019; López-Fernández et al., 2013; Mahe et al., 2014; Siqueira et al., 2020). Specifically in surgeonfishes, studies have investigated the feeding mechanics of herbivores related to body and head movements to understand how these

structures facilitate a specialized feeding mode (Mihalitsis & Wainwright, 2024; Perevolotsky et al., 2020), and differences in head and body shape have been hypothesized to facilitate different feeding modes (Robertson et al., 1979). The smaller mouths and more maneuverable body of benthic herbivores/detritivores may be advantageous in their distinct grazing behavior, while the larger mouths of pelagic planktivores may maximize dietary intake. In fact, this relationship has been discussed in a previous study among many reef fish groups (Claverie & Wainwright, 2014). We see that omnivores do not exhibit an "intermediate" head and body shape, despite these taxa being observed to occupy both trophic niches. One explanation for this result could be that an intermediate shape (say a mid-sized mouth and a body not optimized for either maneuverability or steady swimming) does not perform well at either feeding behavior, making it an unstable morphology in terms of evolutionary fitness. If correct, why then do omnivores tend to exhibit the pelagic planktivore phenotype over the benthic herbivore/detritivore phenotype? This could be because the pelagic planktivore dietary ecotype is more specialized; fishes can be successful herbivores with a larger mouth and elongated bodies, but would be unsuccessful at planktivory with smaller mouths and bodies not optimized for steady swimming performance (Langerhans, 2008).

4.4 Evolutionary correlations between shapes

Significant morphological correlations between morphometric subsets within Acanthuridae indicate that the evolution of one shape may influence the evolution of the other in a complementary pattern. Our results support strong correlations between the caudal and pectoral fins as well as caudal fin shape and body shape. The nearly significant relationship between caudal fin and head shape also suggests that head shape could be a major driver of the

relationship between caudal fin and body shape, but clearly some aspect of the axial body is contributing to the significance of this relationship. Although we elected not to test the association between head and body shape due to overlap in landmarks of each subset, there is evidence they potentially covary across species as elongation ratio is associated with head shape (Figure S8). For the correlations between the caudal and pectoral fins as well as caudal fin shape and body shape, the shared evolutionary histories of species have low explanatory power towards the patterns of covariation we found between shapes. It is likely that other factors, such as diet or the swimming biomechanics of surgeonfishes are driving these correlations.

The correlation between caudal fin and body shape (Figure 9) shows that the omnivores and pelagic planktivores separate from benthic herbivores in PLS1 space. Some omnivorous species also separate from pelagic planktivorous species and move towards benthic herbivores in their dominant section of PLS1 space. This visual pattern contradicts our caudal fin shape analyses, where we found no significant difference between shape and diet, as well as our body shape analyses where we find that omnivores do not exhibit an "intermediate" body shape. This could suggest that not one, but a combination of multiple morphological specializations across the body plan facilitate omnivory in surgeonfishes. McCord et al. (2021) found that both body size and dietary ecotype are significantly associated with patterns of diversification across the damselfishes, and that the highest rates of net diversification are associated with medium body size and pelagic planktivory. If dietary ecotype can influence both body size and rates of evolution, it may have unexplored consequences for the likelihood of ecomorphological covariation; trophic diversity could promote covariation in shapes but ultimately result in similar individual shapes across certain dietary ecotypes. Here, we provide evidence that dietary ecotype could be the driving force behind evolution of covariation in caudal fin and body shapes in

surgeonfishes.

Diet may be driving the covariation between caudal fin and body shape due to functional demands related to feeding behavior. Coordinated movements across fins and bodies facilitate feeding behavior in wrasses and parrotfishes (Rice et al., 2008; Rice & Westneat, 2005), and studies have shown that herbivorous surgeonfishes have unique feeding behaviors that involve coupled movements of the head, body, and fins (Mihalitsis & Wainwright, 2024; Perevolotsky et al., 2020). Considering fin and body shape enable different locomotor modes in fishes (Friedman et al., 2021; Gerstner, 1999; Walker et al., 2013; Walker & Westneat, 2000, 2002), our results present strong evidence that the observed correlation in caudal fin shape and body shape may have arisen to meet the locomotor functional demands related to specific dietary types. Integrated systems score higher in performance landscapes than non-integrated systems, and diet is suggested to be the mechanism of this covariation (Klingenberg, 2013; Sansalone et al., 2022). On the other hand, diet is likely not the cause of the covariation of the caudal and pectoral fin.

Through our combined analyses, further evidence for the evolution of pectoral fin and caudal fin shapes as pairs of low/high AR (Figures 3, 5, 6) can be seen in our PLS results (Figure 10). However, unlike the association between caudal fin and body shape, this correlation does not seem to be associated with dietary ecotype, as distinct dietary ecotypes do not separate in PLS1 space (Figure S9). Acanthurids show a strong inverse relationship between caudal and pectoral fin AR, and we conclude that evolutionary covariation among these propulsive fins is driven by the biomechanical demands of different swimming modes, either labriform or body-caudal-fin mode of propulsion and maneuverability. We also note that the extremes of high pectoral AR or caudal AR, associated with low AR in the other fin, are accompanied by many species that are intermediate for both fins, suggesting that a wide range of fin shapes and

mechanisms are retained in the family and contribute to high morphological diversity in the group.

Morphological integration arising from functional coupling between shapes is expected to promote the evolution of correlations (Olson & Miller 1958; Riedl 1978; Cheverud 1982, 1984; Schlosser & Wagner 2004). Classic thoughts on integration suggest that the connectedness of integrated shapes may be evolutionarily restrictive and prevent rapid diversification in multiple directions, while non-integrated shapes can evolve independently from one another (Wagner & Altenberg 1996). Thus, non-integrates systems may be more likely to promote rapid diversification (Wagner & Altenberg 1996), although this depends on the lability of the structure of integration (Webster & Zelditch 2011). In fact, recent studies have suggested that integration may be related to rapid diversification, especially in fishes (Burns et al., 2023; Evans et al., 2021; Larouche et al., 2018). The integration of shapes thus has implications for overall diversification rates, but what evolutionary patterns emerge when looking at the relationships *between* coupled shapes? Do the ratios of evolutionary rates between shape pairings suggest similar or different rates of evolution, and does this depend on the strength of correlation between shapes? In all but one of our two-block PLS tests, the ratio of evolutionary rates across PLS axes was at least 1.48, suggesting that rates of evolution differ across blocks (Table 3). Our two-block PLS test that showed similar rates of evolution across blocks was our least significant association (lowest p-value and PLS correlation coefficient), although not significantly different in terms of levels of integration compared to the other nonsignificant tests (Table S2). In our significantly correlated shapes, PLS scores related to caudal fin shape exhibited evolutionary rates almost 1.5 to 2.5 times that of PLS scores related to body and pectoral fin shape, respectively. We show then that while morphological shapes are correlated, each morphological subset may be evolving at

different rates. In fact, in every comparison (significant and non-significant) PLS axes related to caudal fin (the block correlated with the most other shapes) always exhibited higher evolutionary rates, with the most dramatic being that of almost 5 times the rate seen in PLS axes related to head shape.

The significantly higher rates of evolution associated with the caudal fin could be due to the behavior and coloration related to surgeonfishes' distinct caudal morphology. Many reef fishes will "flash" their caudal fin by either fluttering or rapidly expanding/contracting their fin as a sexual display to females before spawning or nursery behaviors (Bell, 1983; Kohda et al., 2005; Moyer & Shepard, 1975; Russell, 1971). Additionally, many surgeonfishes are territorial (Nursall 1974; Robertson et al. 1979; Schober and Ditrich 1992) and will use this flashing behavior to protect both feeding and mating territories (Schober and Ditrich 1992; personal observations). In addition, surgeonfishes are unique in their use of modified scales (scalpels) on their caudal peduncles that are used in territorial tail beating displays (Ehrlich and Ehrlich 1982; Schober and Ditrich 1992). Furthermore, these scalpels are diversified in terms of coloration. Coloration of the caudal region across surgeonfishes is incredibly diverse, with extremes like *A. lineatus*, one of the most territorial species of surgeonfishes, camouflaging their scalpel among brightly colored stripes juxtaposed against the less territorial species *A. tennentii* having a scalpel highlighted by a bright blue circle (Robertson et al., 1979; Robertson & Gaines, 1986, personal observations). Specialized tail coloration has evolved within fishes as a means for predator defense (Neudecker, 1989), and future studies looking into specialized caudal color in surgeonfishes related to territoriality could provide insight into how coloration and behavior related to distinctive caudal morphology may be driving these high rates of caudal fin diversification among surgeonfishes.

While the caudal fin is the only shape subset that significantly covaries with more than one shape and is the most distinct in terms of evolutionary rates, understanding whether the evolutionary rate differences are related to the strength of the correlation between shapes remains unknown. Differences in evolutionary rates did not follow a consistent pattern. For example, our lowest evolutionary rate difference was found in our least correlated shapes, but our highest evolutionary rate difference was also found between shapes did not significantly covary with one another. Additionally, while the strongly correlated caudal fin and pectoral fin shapes exhibited the largest difference in evolutionary rates of PLS scores, the strongest association of caudal fin shape and body shape exhibited the second lowest difference in evolutionary rates of PLS scores. We encourage further work in evolutionary morphometrics in fishes and other diverse groups to explore the relationship between evolutionary rates of morphometric change and the strength of associations among PLS scores for various structural regions of organisms with important functional and ecological roles. Our novel methodology described here corrects for the appropriate amount of phylogenetic covariances among species and should be used in these future studies, especially in systems that are not evolving under BM.

4. Conclusion

Our revised, species rich, time-calibrated phylogeny of surgeonfishes provides the backdrop to explore morphological associations and evolution using the full body and flexible fin shapes, focusing on four major subsets of shape: head, body, caudal fin, and pectoral fins. Phylogenetic relationships among species and genera garner strong support and are congruent with our morphological data to some degree, providing clarity to the overall topology of the Acanthuridae phylogeny as well as support for classic taxonomy. Surgeonfish shape diversity is

associated with both dietary ecotype and likely locomotor demands which has likely contributed to surgeonfishes evolving two alternative combinations of fin shape, one with a high AR caudal fin and low AR pectoral fins, and the other with high AR pectoral fins and a low AR caudal fin. Phylogenetic signal is generally low, indicating that the shared evolutionary history of species does not substantially explain major correlations between shapes among surgeonfishes. Likely, this covariation is related to their ecology and behavior; caudal fin and body shape covary and relate to dietary ecotype, whereas the covariation between the caudal fin and pectoral fin shape relates to locomotor mechanics. The caudal fin shape exhibits the highest degree of evolutionary rates and is strongly associated with almost all other shape subsets, demonstrating the importance of investigating the relationship between the rates of morphometric evolution and the strength of association between morphometric shapes.

CRediT authorship contribution statement: **Linnea L. Lungstrom**: Conceptualization, Data curation, Formal analysis, Investigation, Methodology, Visualization, Writing – original draft. **Mireille Farjo**: Conceptualization, Data curation, Investigation, Writing – review & editing. **Ryan Isdonas**: Data curation, Investigation, Writing – review & editing. **Andrew B. George**: Data curation, Investigation, Writing – review & editing. **Mark W. Westneat**: Conceptualization, Data curation, Formal analysis, Funding acquisition, Methodology, Software, Supervision, Visualization, Writing – review & editing.

Declaration of Competing Interest: The authors declare that they have no known competing financial interests or personal relationships that could have appeared to influence the work reported in this paper.

Acknowledgements: Thank you to the staff of the Division of Fishes at the Field Museum (Caleb McMahan, Susan Mochel, and Kevin Swagel) for allowing us access to the collections to take photos of specimens for morphometric analysis. We are also grateful to various other institutional and online databases (Smithsonian National Museum of Natural History, Bishop Museum, FishBase, John E. Randall's and Jeffrey T. Williams' Fish Photos) that contributed photos to our dataset. Special thanks to the CRIOBE marine lab for work in Moorea. Thank you to Graham Slater for discussions about phylogenetic corrections related to morphometric analysis. Special thanks to Lydia Smith, Jillian Henss, and Charlene McCord for gene sequencing work at the Field Museum, supporting this research.

Funding: This research was supported by a U.S. Department of Education Graduate Assistance in Areas of National Need Fellowship and a fellowship from the NIH T32 Training Program in Motor Control to L.L.L, support from the National Science Foundation Graduate Research Fellowship Program and U.S. Department of Education Graduate Assistance in Areas of National Need Fellowship to A.B.G., and National Science Foundation grants 1425049 and 1541547 to M.W.W.

Supplementary Materials

Supplementary Text: Methods, Results, Discussion

Supplementary: **Figures**: Figures S1 - S9

Supplementary Tables: Table S1 (in text) and S2 (FigShare).

Supplementary Data (FigShare): Appendix A (GenBank Sources), Appendix B (Image Sources), Appendix C. Ecological Trait References. Appendix D. Elongation and Fin Aspect Ratio Data.

Supplementary Files (FigShare): Phylogenetic Trees

References.

Adams, D. C., Collyer, M. L., Kaliontzopoulou, A., & Baken, E. K. (2025). *Geomorph: Software for geometric morphometric analyses. R package version 4.0.10* [Computer software]. https://cran.r-project.org/package=geomorph

Aguilar-Medrano, R., Frédérich, B., & Barber, P. H. (2016). Modular diversification of the locomotor system in damselfishes (Pomacentridae). *Journal of Morphology*, *277*(5), 603–614. https://doi.org/10.1002/jmor.20523

Alfaro, M. E., Faircloth, B. C., Harrington, R. C., Sorenson, L., Friedman, M., Thacker, C. E., Oliveros, C. H., Černý, D., & Near, T. J. (2018). Explosive diversification of marine fishes at the Cretaceous–Palaeogene boundary. *Nature Ecology & Evolution*, *2*(4), 688–696. https://doi.org/10.1038/s41559-018-0494-6

Baken, E. K., Collyer, M. L., Kaliontzopoulou, A., & Adams, D. C. (2021). geomorph v4.0 and gmShiny: Enhanced analytics and a new graphical interface for a comprehensive morphometric experience. *Methods in Ecology and Evolution*, *12*(12), 2355–2363. https://doi.org/10.1111/2041-210X.13723

Bejarano, S., Jouffray, J.-B., Chollett, I., Allen, R., Roff, G., Marshell, A., Steneck, R., Ferse, S. C., & Mumby, P. J. (2017). The shape of success in a turbulent world. *Functional Ecology*, *31*(6), 1312–1324.

Bell, L. J. (1983). Aspects of the reproductive biology of the wrasse, Cirrhilabrus temminckii, at Miyake-jima, Japan. *Japanese Journal of Ichthyology*, *30*(2), 158–167. https://doi.org/10.11369/jji1950.30.158

Betancur-R, R., Wiley, E. O., Arratia, G., Acero, A., Bailly, N., Miya, M., Lecointre, G., & Ortí, G. (2017). Phylogenetic classification of bony fishes. *BMC Evolutionary Biology*, *17*(1), 162. https://doi.org/10.1186/s12862-017-0958-3

Borden, W. C. (1998). Phylogeny of the Unicornfishes (Naso, Acanthuridae) Based on Soft Anatomy. *Copeia*, *1998*(1), 104–113. JSTOR. https://doi.org/10.2307/1447705

Bouckaert, R., Vaughan, T. G., Barido-Sottani, J., Duchêne, S., Fourment, M., Gavryushkina, A., Heled, J., Jones, G., Kühnert, D., De Maio, N., Matschiner, M., Mendes, F. K., Müller, N. F., Ogilvie, H. A., du Plessis, L., Popinga, A., Rambaut, A., Rasmussen, D., Siveroni, I., … Drummond, A. J. (2019). BEAST 2.5: An advanced software platform for Bayesian evolutionary analysis. *PLOS Computational Biology*, *15*(4), e1006650. https://doi.org/10.1371/journal.pcbi.1006650

Burns, M. D., Collyer, M. L., & Sidlauskas, B. L. (2023). Simultaneous integration and modularity underlie the exceptional body shape diversification of characiform fishes. *Evolution*, *77*(3), 746–762. https://doi.org/10.1093/evolut/qpac070

Chang, X., Zhang, L., & He, X. (2012). Numerical study of the thunniform mode of fish swimming with different Reynolds number and caudal fin shape. *Computers & Fluids*, *68*, 54–70. https://doi.org/10.1016/j.compfluid.2012.08.004

Claverie, T., & Wainwright, P. C. (2014). A morphospace for reef fishes: Elongation is the dominant axis of body shape evolution. *PloS One*, *9*(11), e112732.

Clements, K. D., Gray, R. D., & Howard Choat, J. (2003). Rapid evolutionary divergences in reef fishes of the family Acanthuridae (Perciformes: Teleostei). *Molecular Phylogenetics and Evolution*, *26*(2), 190–201. https://doi.org/10.1016/S1055-7903(02)00325-1

Collar, D. C., O'Meara, B. C., Wainwright, P. C., & Near, T. J. (2009). Piscivory limits diversification of feeding morphology in centrarchid fishes. *Evolution*, *63*(6), 1557–1573. https://doi.org/10.1111/j.1558-5646.2009.00626.x

Collyer, M. L., & Adams, D. C. (2018). *RRPP: An R package for fitting linear models to high-dimensional data using residual randomization.* [Computer software].

Collyer, M. L., & Adams, D. C. (2024). *RRPP: Linear Model Evaluation with Randomized Residuals in a Permutation Procedure, R package version 2.0.4.* [Computer software].

Cooper, W. J., Carter, C. B., Conith, A. J., Rice, A. N., & Westneat, M. W. (2017). The evolution of jaw protrusion mechanics is tightly coupled to bentho-pelagic divergence in damselfishes (Pomacentridae). *Journal of Experimental Biology*, *220*(4), 652–666. https://doi.org/10.1242/jeb.143115

Cooper, W. J., & Westneat, M. W. (2009). Form and function of damselfish skulls: Rapid and repeated evolution into a limited number of trophic niches. *BMC Evolutionary Biology*, *9*(1), 24. https://doi.org/10.1186/1471-2148-9-24

Drucker, E. G. (1996). The Use of Gait Transition Speed in Comparative Studies of Fish Locomotion1. *American Zoologist*, *36*(6), 555–566. https://doi.org/10.1093/icb/36.6.555

Drummond, A. J., Ho, S. Y. W., Phillips, M. J., & Rambaut, A. (2006). Relaxed Phylogenetics and Dating with Confidence. *PLOS Biology*, *4*(5), e88. https://doi.org/10.1371/journal.pbio.0040088

Drummond, A. J., Nicholls, G. K., Rodrigo, A. G., & Solomon, W. (2002). Estimating Mutation Parameters, Population History and Genealogy Simultaneously from Temporally Spaced Sequence Data. *Genetics*, *161*(3), 1307–1320. https://doi.org/10.1093/genetics/161.3.1307

Du, T. Y., Tissandier, S. C., & Larsson, H. C. E. (2019). Integration and modularity of teleostean pectoral fin shape and its role in the diversification of acanthomorph fishes. *Evolution*, *73*(2), 401–411. https://doi.org/10.1111/evo.13669

Evans, K. M., Larouche, O., Watson, S.-J., Farina, S., Habegger, M. L., & Friedman, M. (2021). Integration drives rapid phenotypic evolution in flatfishes. *Proceedings of the National Academy of Sciences*, *118*(18), e2101330118. https://doi.org/10.1073/pnas.2101330118

Evans, K. M., Waltz, B. T., Tagliacollo, V. A., Sidlauskas, B. L., & Albert, J. S. (2017). Fluctuations in Evolutionary Integration Allow for Big Brains and Disparate Faces. *Scientific Reports*, *7*(1), 40431. https://doi.org/10.1038/srep40431

Feilich, K. L. (2016). Correlated evolution of body and fin morphology in the cichlid fishes. *Evolution*, *70*(10), 2247–2267. https://doi.org/10.1111/evo.13021

Flammang, B. E., & Lauder, G. V. (2013). Pectoral fins aid in navigation of a complex environment by bluegill sunfish under sensory deprivation conditions. *Journal of Experimental Biology*, *216*(16), 3084–3089. https://doi.org/10.1242/jeb.080077

Floeter, S. R., Bender, M. G., Siqueira, A. C., & Cowman, P. F. (2018). Phylogenetic perspectives on reef fish functional traits. *Biological Reviews*, *93*(1), 131–151. https://doi.org/10.1111/brv.12336

Friedman, S. T., Martinez, C. M., Price, S. A., & Wainwright, P. C. (2019). The influence of size on body shape diversification across Indo-Pacific shore fishes*. *Evolution*, *73*(9), 1873–1884. https://doi.org/10.1111/evo.13755

Friedman, S. T., Price, S. A., Hoey, A. S., & Wainwright, P. C. (2016). Ecomorphological convergence in planktivorous surgeonfishes. *Journal of Evolutionary Biology*, *29*(5), 965–978. https://doi.org/10.1111/jeb.12837

Friedman, S. T., Price, S. A., & Wainwright, P. C. (2021). The Effect of Locomotion Mode on Body Shape Evolution in Teleost Fishes. *Integrative Organismal Biology*, *3*(1), obab016. https://doi.org/10.1093/iob/obab016

Fulton, C., Bellwood, D., & Wainwright, P. (2001). The relationship between swimming ability and habitat use in wrasses (Labridae). *Marine Biology*, *139*(1), 25–33. https://doi.org/10.1007/s002270100565

George, A. B., & Westneat, M. W. (2019). Functional morphology of endurance swimming performance and gait transition strategies in balistoid fishes. *Journal of Experimental Biology*, *222*(8), jeb194704. https://doi.org/10.1242/jeb.194704

Gerstner, C. L. (1999). Maneuverability of four species of coral-reef fish that differ in body and pectoral-fin morphology. *Canadian Journal of Zoology*, *77*(7), 1102–1110. https://doi.org/10.1139/z99-086

Ghezelayagh, A., Harrington, R. C., Burress, E. D., Campbell, M. A., Buckner, J. C., Chakrabarty, P., Glass, J. R., McCraney, W. T., Unmack, P. J., Thacker, C. E., Alfaro, M. E., Friedman, S. T., Ludt, W. B., Cowman, P. F., Friedman, M., Price, S. A., Dornburg, A., Faircloth, B. C., Wainwright, P. C., & Near, T. J. (2022). Prolonged morphological expansion of spiny-rayed fishes following the end-Cretaceous. *Nature Ecology & Evolution*, *6*(8), 1211–1220. https://doi.org/10.1038/s41559-022-01801-3

Goswami, A., & Polly, P. D. (2010). The Influence of Modularity on Cranial Morphological Disparity in Carnivora and Primates (Mammalia). *PLOS ONE*, *5*(3), e9517. https://doi.org/10.1371/journal.pone.0009517

Goswami, A., Smaers, J. B., Soligo, C., & Polly, P. D. (2014). The macroevolutionary consequences of phenotypic integration: From development to deep time. *Philosophical*

Transactions of the Royal Society B: Biological Sciences, *369*(1649), 20130254. https://doi.org/10.1098/rstb.2013.0254

Guiasu, R. C., & Winterbottom, R. (1993). Osteological Evidence for the Phylogeny of Recent Genera of Surgeonfishes (Percomorpha, Acanthuridae). *Copeia*, *1993*(2), 300–312. https://doi.org/10.2307/1447130

Hughes, L. C., Ortí, G., Huang, Y., Sun, Y., Baldwin, C. C., Thompson, A. W., Arcila, D., Betancur-R., R., Li, C., Becker, L., Bellora, N., Zhao, X., Li, X., Wang, M., Fang, C., Xie, B., Zhou, Z., Huang, H., Chen, S., … Shi, Q. (2018). Comprehensive phylogeny of ray-finned fishes (Actinopterygii) based on transcriptomic and genomic data. *Proceedings of the National Academy of Sciences*, *115*(24), 6249–6254. https://doi.org/10.1073/pnas.1719358115

Kalyaanamoorthy, S., Minh, B. Q., Wong, T. K. F., von Haeseler, A., & Jermiin, L. S. (2017). ModelFinder: Fast model selection for accurate phylogenetic estimates. *Nature Methods*, *14*(6), 587–589. https://doi.org/10.1038/nmeth.4285

Klanten, S. O., van Herwerden, L., Choat, J. H., & Blair, D. (2004). Patterns of lineage diversification in the genus Naso (Acanthuridae). *Molecular Phylogenetics and Evolution*, *32*(1), 221–235.

Klingenberg, C. P. (2013). Cranial integration and modularity: Insights into evolution and development from morphometric data. *Hystrix*, *24*(1), 43.

Kohda, M., Sasaki, K., Sakai, Y., Ohnishi, N., & Matsumoto, K. (2005). Preliminary study on female choice of mates versus sites in a wrasse, Cirrhilabrus temminckii. *Ichthyological Research*, *52*(4), 406–409. https://doi.org/10.1007/s10228-005-0292-4

Krishnadas, A., Ravichandran, S., & Rajagopal, P. (2018). Analysis of biomimetic caudal fin shapes for optimal propulsive efficiency. *Ocean Engineering*, *153*, 132–142. https://doi.org/10.1016/j.oceaneng.2018.01.082

Langerhans, R. B. (2008). Predictability of phenotypic differentiation across flow regimes in fishes. *Integrative and Comparative Biology*, *48*(6), 750–768.

Larouche, O., Cloutier, R., & Zelditch, M. L. (2015). Head, Body and Fins: Patterns of Morphological Integration and Modularity in Fishes. *Evolutionary Biology*, *42*(3), 296–311. https://doi.org/10.1007/s11692-015-9324-9

Larouche, O., Zelditch, M. L., & Cloutier, R. (2018). Modularity promotes morphological divergence in ray-finned fishes. *Scientific Reports*, *8*(1), 7278. https://doi.org/10.1038/s41598-018-25715-y

López-Fernández, H., Arbour, J. H., Winemiller, K. O., & Honeycutt, R. L. (2013). Testing for ancient adaptive radiations in neotropical cichlid fishes. *Evolution*, *67*(5), 1321–1337. Scopus. https://doi.org/10.1111/evo.12038

Maddison, W. P., & Maddison, D. R. (2025). *Mesquite: A modular system for evolutionary analysis.* (Version 3.70) [Computer software].

Mahe, K., Villanueva, M. C., Vaz, S., Coppin, F., Koubbi, P., & Carpentier, A. (2014). Morphological variability of the shape of striped red mullet Mullus surmuletus in relation to stock discrimination between the Bay of Biscay and the eastern English Channel. *Journal of Fish Biology*, *84*(4), 1063–1073. https://doi.org/10.1111/jfb.12345

McCord, C. L., Nash, C. M., Cooper, W. J., & Westneat, M. W. (2021). Phylogeny of the damselfishes (Pomacentridae) and patterns of asymmetrical diversification in body size

and feeding ecology. *PLOS ONE*, *16*(10), e0258889. https://doi.org/10.1371/journal.pone.0258889

Mihalitsis, M., & Wainwright, P. C. (2024). Feeding kinematics of a surgeonfish reveal novel functions and relationships to reef substrata. *Communications Biology*, *7*(1), 13. https://doi.org/10.1038/s42003-023-05696-z

Minh, B. Q., Schmidt, H. A., Chernomor, O., Schrempf, D., Woodhams, M. D., von Haeseler, A., & Lanfear, R. (2020). IQ-TREE 2: New Models and Efficient Methods for Phylogenetic Inference in the Genomic Era. *Molecular Biology and Evolution*, *37*(5), 1530–1534. https://doi.org/10.1093/molbev/msaa015

Monteiroa, L. R. (2013). Morphometrics and the comparative method: Studying the evolution of biological shape. *Hystrix, the Italian Journal of Mammalogy*, *24*(1), 25–32. https://doi.org/doi:10.4404/hystrix-24.1-6282

Moyer, J. T., & Shepard, J. W. (1975). Notes on the spawning behavior of the wrasse, Cirrhilabrus temminckii. *Japanese Journal of Ichthyology*, *22*(1), 40–42. https://doi.org/10.11369/jji1950.22.40

Nash, C. M., Lungstrom, L. L., Hughes, L. C., & Westneat, M. W. (2022). Phylogenomics and body shape morphometrics reveal recent diversification in the goatfishes (Syngnatharia: Mullidae). *Molecular Phylogenetics and Evolution*, *177*, 107616. https://doi.org/10.1016/j.ympev.2022.107616

Natale, R., & Slater, G. J. (2022). The Effects of Foraging Ecology and Allometry on Avian Skull Shape Vary across Levels of Phylogeny. *The American Naturalist*, *200*(4), E174–E188. https://doi.org/10.1086/720745

Navalón, G., Bright, J. A., Marugán-Lobón, J., & Rayfield, E. J. (2019). The evolutionary relationship among beak shape, mechanical advantage, and feeding ecology in modern birds*. *Evolution*, *73*(3), 422–435. https://doi.org/10.1111/evo.13655

Near, T. J., Eytan, R. I., Dornburg, A., Kuhn, K. L., Moore, J. A., Davis, M. P., Wainwright, P. C., Friedman, M., & Smith, W. L. (2012). Resolution of ray-finned fish phylogeny and timing of diversification. *Proceedings of the National Academy of Sciences*, *109*(34), 13698–13703. https://doi.org/10.1073/pnas.1206625109

Near, T. J., & Thacker, C. E. (2024). Phylogenetic Classification of Living and Fossil Ray-Finned Fishes (Actinopterygii). *Bulletin of the Peabody Museum of Natural History*, *65*(1), 3–302. https://doi.org/10.3374/014.065.0101

Neudecker, S. (1989). Eye camouflage and false eyespots: Chaetodontid responses to predators. *Environmental Biology of Fishes*, *25*(1), 143–157. https://doi.org/10.1007/BF00002208

Olsen, A. M., & Westneat, M. W. (2015). StereoMorph: An R package for the collection of 3D landmarks and curves using a stereo camera set-up. *Methods in Ecology and Evolution*, *6*(3), 351–356. https://doi.org/10.1111/2041-210X.12326

Orme, D., Freckleton, R., Thomas, G., Petzoldt, T., Fritz, S., Isaac, N., & Pearse, W. (2025). caper: Comparative Analyses of Phylogenetics and Evolution in R. R package version 1.0.4, https://CRAN.R-project.org/package=caper.

Pennell, M. W., Eastman, J. M., Slater, G. J., Brown, J. W., Uyeda, J. C., FitzJohn, R. G., Alfaro, M. E., & Harmon, L. J. (2014). geiger v2.0: An expanded suite of methods for fitting macroevolutionary models to phylogenetic trees. *Bioinformatics*, *30*(15), 2216–2218. https://doi.org/10.1093/bioinformatics/btu181

Perevolotsky, T., Martin, C. H., Rivlin, A., & Holzman, R. (2020). Work that body: Fin and body movements determine herbivore feeding performance within the natural reef environment. *Proceedings of the Royal Society B*, *287*(1938), 20201903.

Price, S. A., Friedman, S. T., Corn, K. A., Martinez, C. M., Larouche, O., & Wainwright, P. C. (2019). Building a Body Shape Morphospace of Teleostean Fishes. *Integrative and Comparative Biology*, *59*(3), 716–730. https://doi.org/10.1093/icb/icz115

R Core Team. (2024). R: A Language and Environment for Statistical Computing. R Foundation for Statistical Computing, Vienna, Austria. https://www.R-project.org/.

Rambaut, A., Drummond, A. J., Xie, D., Baele, G., & Suchard, M. A. (2018). Posterior Summarization in Bayesian Phylogenetics Using Tracer 1.7. *Systematic Biology*, *67*(5), 901–904. https://doi.org/10.1093/sysbio/syy032

Revell, L. J. (2010). Phylogenetic signal and linear regression on species data. *Methods in Ecology and Evolution*, *1*(4), 319–329. https://doi.org/10.1111/j.2041-210X.2010.00044.x

Revell, L. J. (2024). phytools 2.0: An updated R ecosystem for phylogenetic comparative methods (and other things). *PeerJ*, *12*, e16505. https://doi.org/10.7717/peerj.16505

Ribeiro, E., Davis, A. M., Rivero-Vega, R. A., Ortí, G., & Betancur-R, R. (2018). Post-Cretaceous bursts of evolution along the benthic-pelagic axis in marine fishes. *Proceedings of the Royal Society B: Biological Sciences*, *285*(1893), 20182010. https://doi.org/10.1098/rspb.2018.2010

Rice, A. N., Cooper, W. J., & Westneat, M. W. (2008). Diversification of coordination patterns during feeding behaviour in cheiline wrasses. *Biological Journal of the Linnean Society*, *93*(2), 289–308. https://doi.org/10.1111/j.1095-8312.2007.00915.x

Rice, A. N., & Westneat, M. W. (2005). Coordination of feeding, locomotor and visual systems in parrotfishes (Teleostei: Labridae). *Journal of Experimental Biology*, *208*(18), 3503–3518.

Robertson, D. R., & Gaines, S. D. (1986). Interference Compoetition Structures Habitat Use in a Local Assemblage of Coral Reef Surgeonfishes. *Ecology*, *67*(5), 1372–1383. https://doi.org/10.2307/1938693

Robertson, D. R., Polunin, N. V. C., & Leighton, K. (1979). The behavioral ecology of three Indian Ocean surgeonfishes (Acanthurus lineatus, A. leucosternon and Zebrasoma scopas): Their feeding strategies, and social and mating systems. *Environmental Biology of Fishes*, *4*(2), 125–170. https://doi.org/10.1007/BF00005448

Russell, B. C. (1971). Underwater observations on the reproductive activity of the demoiselleChromis dispilus (Pisces: Pomacentridae). *Marine Biology*, *10*(1), 22–29. https://doi.org/10.1007/BF02026762

Sambilay, V. C. (1990). Interrelationships between swimming speed, caudal fin aspect ratio and body length of fishes. *Fishbyte*, *8*(3), 16–20.

Sansalone, G., Paolo, C., Riccardo, C., Stephen, W., Silvia, C., & Pasquale, R. (2022). Trapped in the morphospace: The relationship between morphological integration and functional performance. *Evolution*, *76*(9), 2020–2031. https://doi.org/10.1111/evo.14575

Schakmann, M., & Korsmeyer, K. E. (2023). Fish swimming mode and body morphology affect the energetics of swimming in a wave-surge water flow. *Journal of Experimental Biology*, *226*(6), jeb244739. https://doi.org/10.1242/jeb.244739

Siqueira, A. C., Morais, R. A., Bellwood, D. R., & Cowman, P. F. (2020). Trophic innovations fuel reef fish diversification. *Nature Communications*, *11*(1), 2669. https://doi.org/10.1038/s41467-020-16498-w

Sorenson, L., Santini, F., Carnevale, G., & Alfaro, M. E. (2013). A multi-locus timetree of surgeonfishes (Acanthuridae, Percomorpha), with revised family taxonomy. *Molecular Phylogenetics and Evolution*, *68*(1), 150–160. https://doi.org/10.1016/j.ympev.2013.03.014

Tavera, J., Acero P., A., & Wainwright, P. C. (2018). Multilocus phylogeny, divergence times, and a major role for the benthic-to-pelagic axis in the diversification of grunts (Haemulidae). *Molecular Phylogenetics and Evolution*, *121*, 212–223. https://doi.org/10.1016/j.ympev.2017.12.032

Wagner, G. P., & Altenberg, L. (1996). Perspective: Complex Adaptations and the Evolution of Evolvability. *Evolution*, *50*(3), 967–976. JSTOR. https://doi.org/10.2307/2410639

Wainwright, P. C., Bellwood, D. R., & Westneat, M. W. (2002). Ecomorphology of Locomotion in Labrid Fishes. *Environmental Biology of Fishes*, *65*(1), 47–62. https://doi.org/10.1023/A:1019671131001

Walker, J. A., Alfaro, M. E., Noble, M. M., & Fulton, C. J. (2013). Body Fineness Ratio as a Predictor of Maximum Prolonged-Swimming Speed in Coral Reef Fishes. *PLOS ONE*, *8*(10), e75422. https://doi.org/10.1371/journal.pone.0075422

Walker, J. A., & Westneat, M. W. (2000). Mechanical performance of aquatic rowing and flying. *Proceedings of the Royal Society of London. Series B: Biological Sciences*, *267*(1455), 1875–1881. https://doi.org/10.1098/rspb.2000.1224

Walker, J. A., & Westneat, M. W. (2002). Performance limits of labriform propulsion and correlates with fin shape and motion. *Journal of Experimental Biology*, *205*(2), 177–187. https://doi.org/10.1242/jeb.205.2.177

Webb, Paul W. 1982. Locomotor Patterns in the Evolution of Actinopterygian Fishes. *American Zoologist* 22 (2): 329–42. https://doi.org/10.1093/icb/22.2.329.

Webb, P. W. (1984). Form and Function in Fish Swimming. *Scientific American*, *251*(1), 72–83. JSTOR.

Weihs, D. 1973. The Mechanism of Rapid Starting of Slender Fish. *Biorheology* 10 (3): 343–50. https://doi.org/10.3233/BIR-1973-10308.

Westneat, M. W. (1996). Functional Morphology of Aquatic Flight in Fishes: Kinematics, Electromyography, and Mechanical Modeling of Labriform Locomotion1. *American Zoologist*, *36*(6), 582–598. https://doi.org/10.1093/icb/36.6.582

Westneat, M. W., Aiello, B. R., Olsen, A. M., & Hale, M. E. (2017). Bioinspiration from flexible propulsors: Organismal design, mechanical properties, kinematics and neurobiology of pectoral fins in labrid fishes. *Marine Technology Society Journal*, *51*(5), 23–34.

Westneat, M., & Wainwright, S. (2001). Mechanical design for swimming: Muscle, tendon, and bone. *Fish Physiology*, *19*, 271–311. https://doi.org/10.1016/S1546-5098(01)19008-4

Winterbottom, R. (1993). Myological Evidence for the Phylogeny of Recent Genera of Surgeonfishes (Percomorpha, Acanthuridae), with Comments on the Acanthuroidei. *Copeia*, *1993*(1), 21–39. JSTOR. https://doi.org/10.2307/1446292